CHALMERS

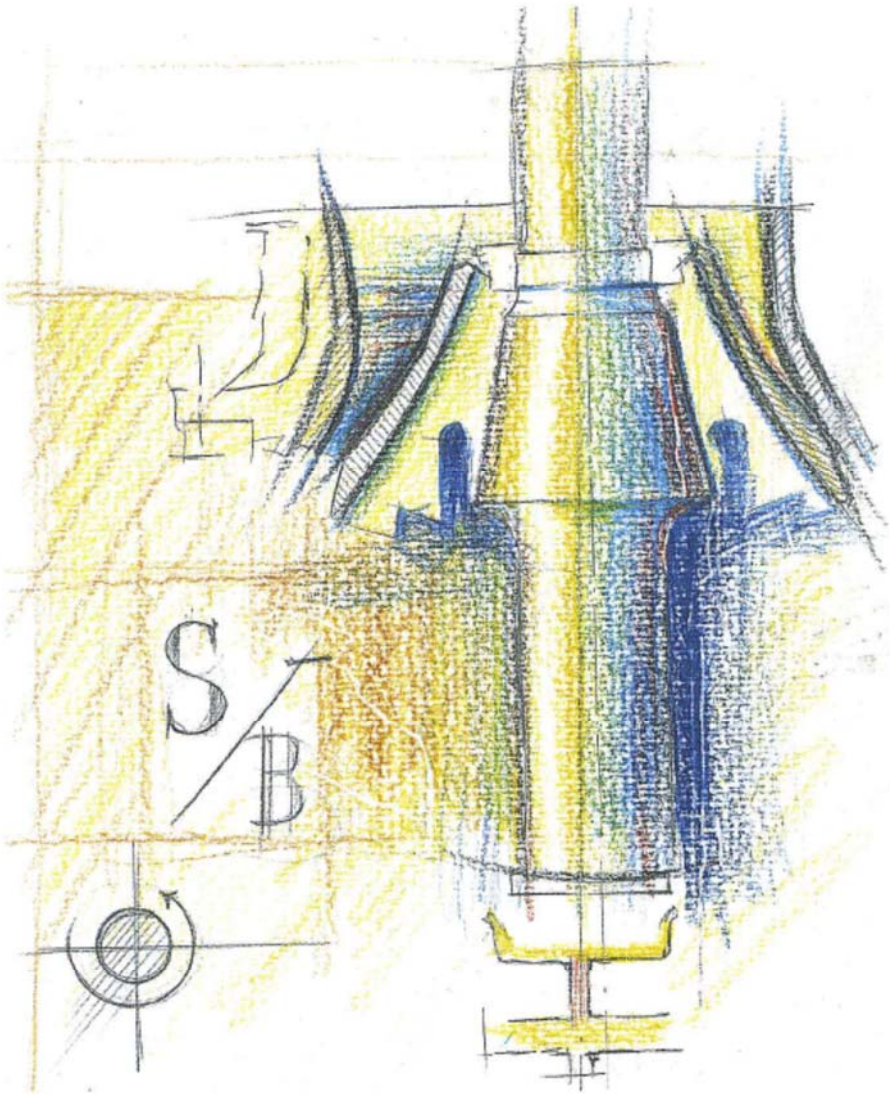

Cone Crusher Performance

CARL MAGNUS EVERTSSON

Department of Machine and Vehicle Design
CHALMERS UNIVERSITY OF TECHNOLOGY
Göteborg, Sweden 2000

CHALMERS UNIVERSITY OF TECHNOLOGY
SE-412 96 Göteborg, Sweden
Telephone. +46-(0)31 772 10 00
www.chalmers.se

Cone Crusher Performance

Cone crushers are used by both aggregate producers and the mining industry. The purpose is to reduce particle size of rock materials or to liberate valuable minerals from ores. A tremendous amount of material is yearly crushed by cone crushers. Despite this fact, the detailed knowledge of *how* a cone crusher works from a process point of view is limited. In order to achieve significant advances in crushing efficiency, increased knowledge is needed. High quality knowledge can only be gained through fundamental understanding.

In this thesis a model for prediction of cone crusher performance is presented. The model can be used as a simulation tool to assist in the design process of crushers. Any arbitrary design can then be studied. If a set of simulations are performed for a given crusher, a *Crusher Performance Map* is achieved which can be used when optimizing a given crushing task or a crushing plant.

THESIS FOR THE DEGREE OF DOCTOR OF PHILOSOPHY

CONE CRUSHER PERFORMANCE

CARL MAGNUS EVERTSSON

MACHINE AND VEHICLE DESIGN
CHALMERS UNIVERSITY OF TECHNOLOGY
GÖTEBORG, SWEDEN 2000

Cone Crusher Performance
Carl Magnus Evertsson
ISBN 91-7197-856-9

Doktorsavhandlingar vid Chalmers tekniska högskola
Ny serie nr 1551
ISSN 0346-718X

Machine and Vehicle Design
Chalmers University of Technology
SE-412 96 Göteborg
Sweden
Telephone + 46 (0)31-772 1000
URL www.chalmers.se

Cover:
Vertical cross-section of a cone crusher by Peter Schachinger

Printed in Sweden by
Chalmers Reproservice
Göteborg, 2000

To Maria and Alice

CONE CRUSHER PERFORMANCE

CARL MAGNUS EVERTSSON
MACHINE AND VEHICLE DESIGN
CHALMERS UNIVERSITY OF TECHNOLOGY

ABSTRACT

Cone crushers are used by both the aggregate producing and the mining industry. Both industries are interested in increasing the product quality while at the same time lowering the production costs. Prediction of crusher performance has been focused on, since crushing is a vital process for both industries.

In this thesis a method for prediction of cone crusher performance is presented. The model is based on the laws of mechanics and constitutive relations concerning rock breakage characteristics. There are some crucial assumptions which are of central interest for the model. The validity of these assumptions has been verified by full-scale tests.

The overall size reduction process is a result of several subsequent crushing events. Therefore, the process occurring in a cone crusher must also be modelled in the same repetitive way. Each crushing event is modelled with a selection and a breakage function. Selection corresponds to the probability of a particle being broken when an aggregate of particles is compressed. Breakage represents the way a single particle is broken into smaller fragments.

The appearance of the selection and breakage functions is rock material specific and can be obtained by laboratory tests. The characterization of the fragmentation behaviour for rock materials is done by form conditioned compression crushing tests. Two modes of breakage are possible to achieve in a cone crusher. The location of the choke level is the criterion which determines the breakage mode. Interparticle breakage is achieved above the choke level while only single particle breakage is achieved below this level.

The crusher model takes the fragmentation behaviour of the rock and feed size distribution into consideration. Moreover, chamber and machine geometry together with machine parameters such as closed side setting, stroke and eccentric speed, is accounted for. On all occasions continuity of mass is preserved.

Three *main factors* are identified to promote the size reduction process occurring in a cone crusher. These factors are: breakage modes, number of crushing zones and compression ratio. The main factors are affected by both design and operating parameters. For a given crusher, the factors depend on eccentric speed, closed side setting, rock material breakage characteristics and feed size distribution. The main factors provide a fundamental and detailed understanding of how a cone crusher operates. Any design consideration should be evaluated against these main factors.

The model can be used as a simulation tool to assist in the design process of crushers. Any arbitrary design can then be studied. If a set of simulations is performed for a given crusher, a *Crusher Performance Map* is achieved, which in turn can be used when optimizing a given crushing task or a crushing plant.

Keywords: aggregates, comminution, crushing, mining, modelling, particle size, simulation, size-reduction.

DISSERTATION

This dissertation comprises the following papers:

Paper A: Evertsson, C. M., “Prediction of Size Distributions from Compressing Crusher Machines”, *Proceedings EXPLO 95 Conference*, Brisbane, Australia, 173-180, 4-7 September 1995.

Paper B: Evertsson, C. M. and Bearman, R. A., “Investigation of Interparticle Breakage as Applied to Cone Crushing”, *Minerals Engineering*, Vol. 10, 199-214, February 1997.

Paper C: Evertsson, C. M., “Output Prediction of Cone Crushers”, *Minerals Engineering*, Vol. 11 215-232, March 1998.

Paper D: Evertsson, C. M., “Modelling of Flow in Cone Crushers”, *Minerals Engineering*, Vol. 12, 1479-1499, December 1999.

Paper E: Evertsson, C. M., “Size Reduction in Cone Crushers”, *Minerals Engineering Conference '99*, Falmouth, England, 22-24 September 1999 (*Accepted for publication in Minerals Engineering*).

DIVISION OF WORK BETWEEN AUTHORS

Paper B:
The draft paper was written by Evertsson and revised by Dr. R. A. Bearman.

CONTENTS

ACKNOWLEDGEMENTS

The initiative for this research project was taken by producers of aggregates, contractors and manufactures of crushing equipment in Scandinavia. The work has been carried out at Machine and Vehicle Design, Chalmers University of Technology.

I wish to express my sincere thanks Professor Göran Gerbert for his excellent supervision. With his great devotion and general competence, Professor Gerbert has supported, inspired and encouraged me throughout the project.

The promoters (also financial sponsors of the project) formed a technical reference group to which the author has regularly reported and presented research results. The people who has been working in the reference are (in alphabetical order, past and present): Jonas Andersson (Nordberg Sweden AB), Per Andersson (SveBeFo), Richard Bern (Svedala-Arbrå AB), Jan Bida (NCC Industri AB), Hans Carlsson (Sabema Material AB), Kjell Carlsson (Sabema Material AB), Leif Dahlqvist (Skanska AB), Konny Deubler (Råsjö Kross AB), Christer Hagert (Vägverket), Pär Johnning (Ballast Väst AB), Christian Ottergren (Svedala Industri AB), Lennart Persson (Skanska AB), Bo Ronge (Chalmers University of Technology), Sigvard Sundelid (Gatu & Väg AB) and Sven-Olof Wennberg (Nordberg Sweden AB). Each member of the technical reference group is hereby gratefully acknowledged.

The author is grateful to the following companies and organizations for funding this work: Development Fund of the Swedish Construction Industry (SBUF), Gatu & Väg AB, National Swedish Road Administration (Vägverket), National Swedish Sand and Crushed Stone Association (GMF), NCC Baggermanns AB, Nordberg Sweden AB, Råsjö Kross AB, Sabema Material AB, Skanska AB and Svedala Industri AB.

I would like to thank all my colleagues (past and present) at Machine and Vehicle Design. They have all, in some way, contributed to the progress of my work.

Dr. Anders Hedman deserves special thanks for reading the thesis and many of the papers. During the years Anders has been helpful in increasing my vocabulary and among other things taught me that Gothenburg is a city in Nebraska.

Finally, I want to express my gratitude to Maria for her love and for having the patience of an angel with me. I must also thank our daughter Alice for being there with her exultingly happiness and always ready to jump for joy.

Carl Magnus Evertsson

Göteborg, January 2000

1 INTRODUCTION

Cone crushers are used by both aggregate producers and the mining industry. The purpose of using crushers is to reduce the particle size of rock materials or to liberate valuable minerals from ores. A tremendous amount of material is crushed yearly by cone crushers. Despite this fact, the detailed knowledge of *how* a cone crusher works from a process point of view is quite poor. In order to achieve significant advances in crushing efficiency, increased knowledge is needed. High quality knowledge can only be gained through fundamental understanding.

1.1 PRODUCTION OF BALLAST MATERIAL

Crushers are of central importance for the production of aggregates from rock material as it is in the crushers that the product is actually produced. The important crushing aspects for the aggregate producers are to increase the product quality and capacity while at the same time lowering the production costs.

During the last few years the quality requirements on roads and railroads have become more accentuated, owing to the desire to minimise maintenance costs. In turn, this has led to increasing requirements in the preparation of ballast materials and pavement aggregates. No longer can the quarry operator offer either quality or quantity – both are now required. Owing to lack of availability and to legal restrictions, access to natural gravel in northern Europe is decreasing. The use of crushed rock material is therefore becoming more and more important.

The total annual consumption of ballast material in Sweden has varied between 65 and 100 million tons during the nineties. The relative amount of crushed rock is increasing steadily and was approximately around 50% in 1999. The consumption of natural gravel is decreasing. Production of crushed rock material comprises drilling, blasting, crushing and screening. Sometimes it is claimed that crushing is the most important production step, because the final product is formed in the crushers.

Crushed ballast material is produced in two main consecutive steps where the particles are formed, viz. blasting and crushing. The raw material for the process is solid rock. The purpose of blasting is primarily to liberate the material from the surrounding rock and secondarily to reduce its handling size.

After blasting, the rock material is transported to a crushing plant, often situated near the pit. Crushing plants have very different layouts depending on when and for what purpose they were built. The properties of the rock material, together with the type of product and capacity demand, are factors that influence the choice of crushers and crushing plant layout.

An example of a crushing plant is shown in Figure 1. In the first step, feeder and grizzly, of the process an important quality improvement takes place. Soil, clay and fines are separated from the rock of higher quality. The fine material originating from weak zones in the rock mass would otherwise pass through several process steps, with unnecessary and undesirable waste in capacity. If the weaker material is allowed to be added to the final product, a significant decrease in product quality appears.

Today, there is no technology available from which the total size reduction of all the demanded product gradings can be achieved in one single step. Consequently, crushing is performed as a series of consecutive process steps. By screening, ready-made gradings are separated at intermediate and final stages. Correctly explored, product quality increases with the number of crushing steps. Repeated size reduction improves the quality and strength gradually at every stage. Gentle crushing, i.e. small size reduction in the last stage, is known to give a product with high strength and a good particle shape, i.e. high cubicity.

The primary crusher is normally a jaw crusher which is fed with blasted rock material. As the size of the blasted material may vary greatly, the primary crusher has to have a large inlet opening. Secondary crushers are normally of the cone or gyratory type. Tertiary and final crushers are mostly cone crushers. In situations where very high cubicity is required, the final crusher may alternatively be an impact crusher if the rock is particularly difficult to shape.

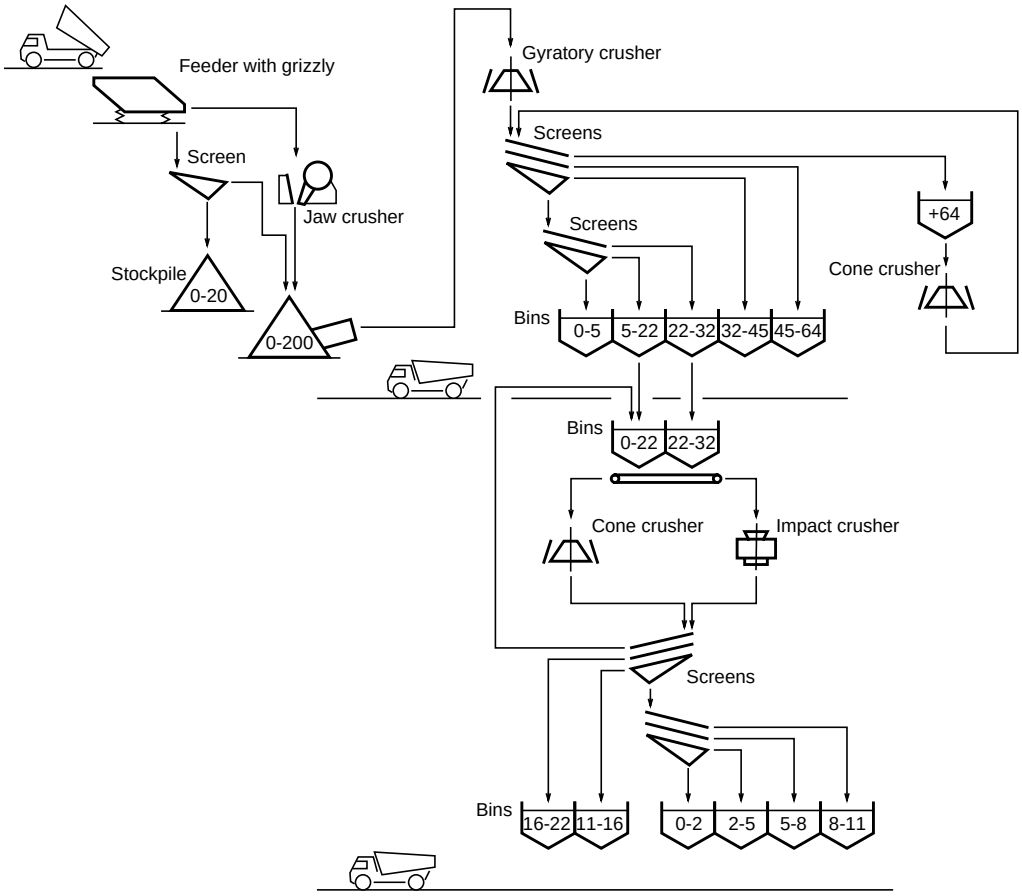

Figure 1. Layout of a four-stage crushing plant for ballast production.

1.2 CRUSHING OF MINERAL ORES

In the mining industry crushing is the first mechanical stage in the process of comminution, in which the main objective is the liberation of valuable minerals from the gangue. The most important crushing aspect is normally the reduction ratio, which is an implicit measure of the product size distribution.

A layout of a size reduction plant for comminution of a nickel rich ore is shown in Figure 2. The plant consists of three crushing stages and one single milling stage. Only one product is required from the crushing plant. That product is then the feed to the milling stage. After milling the material is fed to a concentration plant.

The primary crusher is normally a gyratory or a jaw crusher, depending on the capacity requirement. Gyratory crushers have significantly higher throughput than jaw crushers. This is the reason why gyratory crushers are commonly used as primary crushers by the mining industry. Primary crushing can be performed underground in the mine or on the surface close to the subsequent crushing and comminution stages.

Secondary crushers can be of the gyratory or cone type. Tertiary crushers are almost

exclusively cone crushers. The configuration of secondary and tertiary crushers together with screens varies from case to case. Closed circuits are very common where the crushers are producing a ball mill feed. For closed circuit crushing the finished product is the undersize from the screens while the oversize material is fed back to the crushers and recrushed. Open circuit crushing is often used in intermediate crushing stages, or when the secondary crushing plant is producing a rod mill feed.

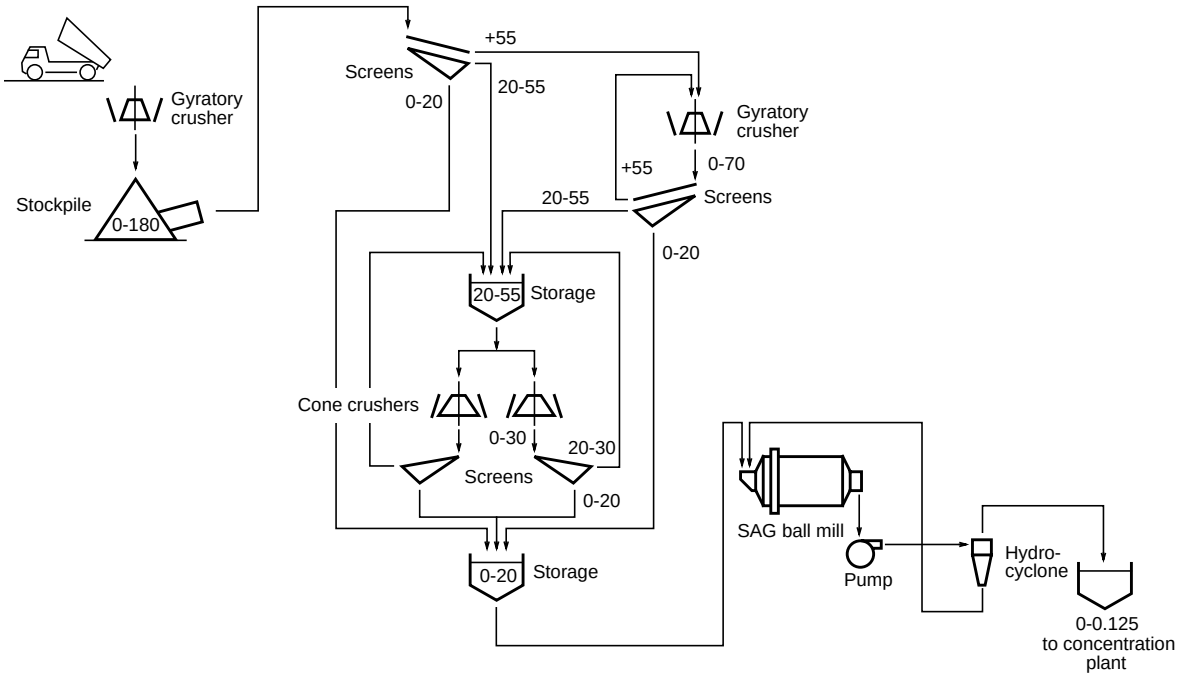

Figure 2. Layout of a size reduction circuit for a nickel rich ore.

1.3 BASIC COMMINUTION PRINCIPLES

There are three comminution principles of industrial interest. Other possible principles exist (electrical etc.) but to date these have not reached the level required for commercial applications. The basic comminution principles described here are:

- Compressive crushing
- Impact crushing
- Attrition

All important minerals and rock materials are crystalline. In a crystalline structure the atoms are ordered in a regular three-dimensional pattern. To reduce the particle size of a rock material we have to divide each particle into smaller particles. For a given volume of material, the total surface area must increase as the number of particles increases. The increase of the overall surface area is a process which is energy consuming.

During compression, energy is transformed from potential energy into elastic energy, which is stored in the crystal lattice. When the stress level somewhere in a crystal reaches a critical value, the interatomic bonds will be broken and a crack will propagate. The stress concentration depends on the mechanical properties of the individual materials, but most important is normally the presence of cracks or flaws in the matrix. These cracks and flaws will act as sites for the stress concentration and from these sites the cracks will propagate. When a crack propagates, a new surface will be created. As an atom on a free surface has a higher potential compared to an atom in the matrix, the creation of a free surface will be an

energy consuming process. A part of the elastically stored energy will transform into surface energy as the crack propagates. The rest of the elastic energy will dissociate as the crystal relaxes. This behaviour is known as brittle fracture. In contrast, a tough and ductile material, as for example steel, can relax the elastic energy by the mechanism of plastic flow. The energy is then consumed in distorting the shape of the material.

1.3.1 COMPRESSIVE CRUSHING

In compressing crushers the rock material is crushed by squeezing the particles between two surfaces. By compression of the material, contact forces between the particles give rise to a tensile stress field within the rock particles. Cracks are formed when the stress field at some local point exceeds a critical value. When the cracks propagate or link together by brittle rupture, a macroscopic breakage is achieved which results in smaller fragments.

Compressive crushing can be either *force* or *form conditioned*. For the force conditioned case the displacement, and thus the size reduction, is a function of the applied force. By controlling the force, and implicitly also the energy input, the size reduction can be controlled. In the form conditioned case, the size reduction and the applied force are a function of the displacement. Size reduction can be controlled by controlling the compression. Energy input and the resulting force are secondary parameters in the form conditioned case.

Jaw, gyratory, cone and roller crushers are all examples of crusher machines that utilize form conditioned compression to achieve size reduction. There is an essential and important difference between roll crushers and the other crusher types. In a roll crusher the material is only compressed once while, for example, in a cone crusher the size reduction is a repetitive process.

A particle which is broken by compressive crushing generates daughter fragments that fall into two main size classes. A discrete number of larger fragments are formed by cracking as a consequence of the tensile stress state. Some amount of fine material is generated at the contact points due to shear stresses.

1.3.2 IMPACT CRUSHING

Another commonly used fragmentation principle is impact breakage. Impact breakage is an energy controlled form of breakage. The energy can be transmitted to the particles by a rotor which accelerates the particles to a velocity close to the peripherical speed of the rotor. The particles are then let to impact with a wall of other particles where the fragmentation occurs, see Figure 3. The amount of size reduction obtained is controlled by the amount of energy transmitted to the particles. The kinetic energy is in turn dependent on the particle velocity. The size reduction can therefore be controlled by the speed of the rotor.

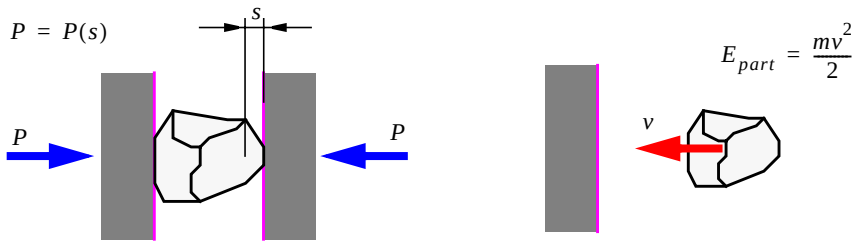

Figure 3. The main difference between form conditioned (left) and energy conditioned (right) breakage is the principle for energy input.

Crushing machines utilizing energy controlled breakage are called impact crushers. These

types of crusher are known to produce a product with a good particle shape, i.e. high cubicity. Depending on the energy level, the crusher can be used to primarily improve shape or to give significant size reduction. A drawback of impact crushers is that they produce a significant amount of fines. This property is a direct consequence of the utilized comminution principle.

From strength tests utilizing a modified Hopkinson Pressure Bar, Briggs and Bearman [4] concluded that impact crushers produce material that contains less variation in strength than the feed because every particle is exposed to the breakage mechanism. Cone crushers do not break material as consistently as impact crushers, as there is variation in both the number of particles exposed to the breakage mechanism and the degree to which the particles are crushed.

1.3.3 ATTRITION

Attrition is breakage by shear failure and produces mostly fine material. Generation of fines is often undesirable. Attrition occurs mainly in practice due to interaction between particles and is thus to be considered as interparticle breakage.

1.4 OPERATING PRINCIPLE OF CONE CRUSHERS

In a cone crusher the rock material is crushed between rigid surfaces. The motion of the moving surface is independent of the loading of the crusher. Therefore, the explored comminution principle is form conditioned compressive crushing.

There is no significant difference between cone and gyratory crushers. In both types, the crushing action is achieved by an eccentric gyratory movement of the main shaft axis, as shown in Figure 4. Particles are nipped, compressed and crushed between mantle and concave. Breakage of particles can be both *single particle* (particles are broken between cone and mantle) and *interparticle* (between other particles). The mantle and the concave must be replaced regularly as they are continuously subjected to wear.

Crushing takes place continuously and is interparticle to a great extent. Interparticle crushing is achieved when a particle is stressed and broken between other particles. Interparticle breakage is desirable from the point of view of wear and service life. Interparticle breakage is also considered to give the best shape of the produced particles. To achieve interparticle breakage *choke fed* conditions are normally recommended. Choke fed conditions imply that the inlet of the crusher is covered with feed material. The feed material is then fed into the crusher by the influence of gravity.

The basic operating principle of a cone crusher is shown in Figure 4. The properties, i.e. size distribution and quality parameters, of the product leaving the crusher are a result of the interaction between crusher and rock material. In turn, the interaction is dependent on chamber geometry, crusher dynamics and rock material characteristics.

Concave, mantle, eccentricity and location of the pivot point together form the chamber geometry of the cone crusher. Like a crank, the eccentricity turns the main shaft with constant speed. At the top the main shaft is journalled in a pivot point. For some designs, the pivot point is just virtual. The mantle is fixed to the main shaft and the concave to the crusher frame. The resulting motion of the mantle and main shaft will be a nutating motion.

If a vertical cross-section of the crusher is considered, the mantle will move cyclically forwards and backwards relatively to the fixed concave. During the squeezing motion the intervening rock material will be subjected to a compressive stress field and thereby comminuted. During the releasing motion the material is able to flow down through the chamber. The motion is driven by the influence of gravity and is governed by the motion of the mantle.

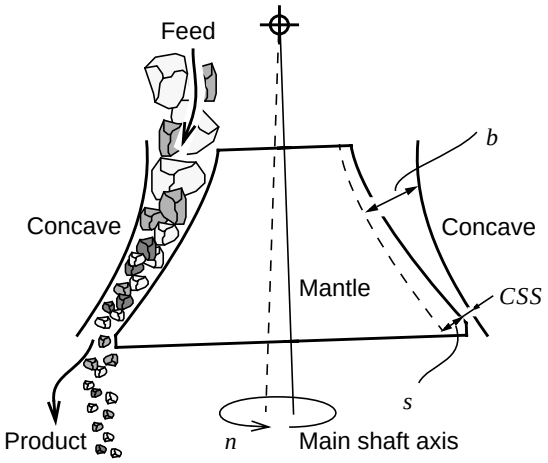

Figure 4. Principle of a cone or gyratory crusher.

At a fixed point of location somewhere in the crusher chamber, the distance between mantle and concave will vary between open and closed position, as shown in Figure 5. The motion can be described with a cyclic function of the eccentric angle α. The eccentric angle corresponds to the position of the eccentricity and therefore also to the position of the main shaft.

The distance between the mantle and concave at the outlet of the crushing chamber is called the *Closed Side Setting* when the mantle is in its closed position. The closed side setting is commonly referred to as the *CSS*.

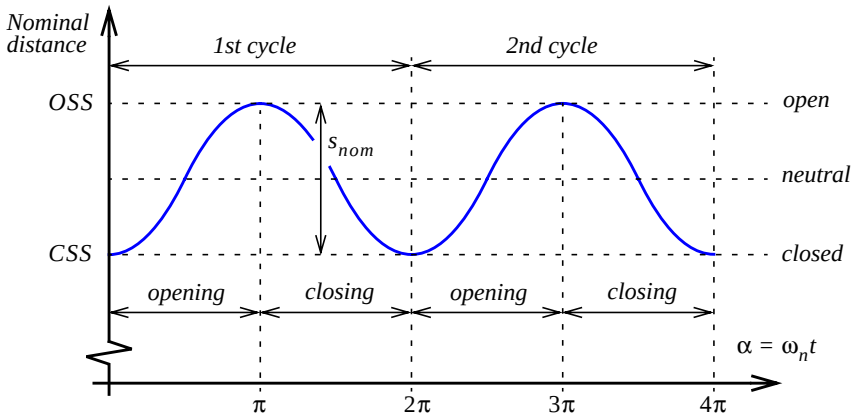

Figure 5. For a fixed point in the chamber the distance between mantle and concave varies cyclically with time.

The breakage of material in cone type gyratory crushers is traditionally regarded as relying upon single particle breakage. In the last ten years the emphasis has shifted with manufacturers trying to generate higher degrees of interparticle breakage. Increasing the degree of interparticle crushing is claimed to improve crushing efficiency and product shape.

When the material passes the crusher it will be subjected to several repeated compressions due to the cyclic oscillation. During every compression the material will be partly crushed. Due to the downward flow and the repeated compressions of the crusher chamber, the material will follow a step-wise motion.

1.5 PROBLEMS

At a first glance a cone crusher may seem to be a quite simple piece of equipment – rocks are reduced in size by passing a machine with moving surfaces. This opinion might be true if no requirements whatsoever are put on either the crushed product or the operation efficiency of the crusher. By applying strictly defined requirements on product quality in combination with a desire to optimize important production aspects, the need for a detailed understanding of crusher operation arises.

The size reduction process occurring in a cone crusher has not yet been fully understood. However, the possibility to simulate and predict cone crusher performance is of great interest for the development of crushers as well as for the design and optimization of crushing plants. A model giving manufacturers the possibility to tailor make a rock crusher to specific customer needs would undoubtedly be a major breakthrough for the quarrying and mining industry.

The problems related to cone crushers can be divided into three different groups. These groups are:

- Process design of crushing plants
- Crusher design
- Crusher operation

1.5.1 PROCESS DESIGN OF CRUSHING PLANTS

When designing comminution processes it is of course of great interest to have knowledge about the different components and machines involved.

The performance of existing crushers can be mapped by full-scale tests. These multi-dimensional maps can then be used for flowsheet simulations to evaluate different process designs. By applying suitable optimization methods it would be possible to obtain the optimal choice of operational parameters for the crushers involved. The disadvantage of this approach is obvious, as full-scale testing can be very time consuming.

1.5.2 CRUSHER DESIGN

The size reduction process occurring in a cone crusher is complex by nature. There are no direct correlations between input and output parameters. If no models are available the possibility to predict the performance of an arbitrary cone crusher is very limited. Therefore, developments and advances in crusher design will be restricted to incremental improvements of existing equipment.

The parameters related to the crusher can be divided into independent and dependent parameters. Independent machine parameters are eccentric speed, closed side setting (CSS), stroke and crushing chamber design. The inherent material properties such as strength and attrition resistance are also to be considered as independent. Feed size, shape and strength are results from previous process stages and therefore treated as independent. The dependent parameters correspond to the output of the crusher. Crusher related parameters are capacity, power requirement and hydraulic pressure (resultant vertical load). Dependent parameters characterizing the product are product size, shape and strength. The dependent parameters are, in one way or another, dependent on at least one independent parameter.

A way to illustrate the dependencies between the independent input parameters and the crushing result is to formulate a so-called interdependency matrix. This matrix relates the input to the output parameters, as shown in Eq. (1).

$$\begin{bmatrix} \text{Capacity} \\ \text{Power requirement} \\ \text{Hydraulic pressure} \\ \text{Product size} \\ \text{Product shape} \\ \text{Product strength} \end{bmatrix} = \begin{bmatrix} X & X & X & X & 0 & 0 & X & 0 & 0 \\ X & X & X & X & X & X & X & X & X \\ X & X & X & X & X & X & X & X & X \\ X & X & X & X & X & X & X & X & X \\ X & X & X & X & 0 & 0 & X & X & X \\ X & X & X & X & X & X & 0 & 0 & X \end{bmatrix} \begin{bmatrix} \text{Speed} \\ \text{CSS} \\ \text{Stroke} \\ \text{Chamber design} \\ \text{Material strength} \\ \text{Attrition resistance} \\ \text{Feed size} \\ \text{Feed shape} \\ \text{Feed strength} \end{bmatrix} \quad (1)$$

An *X* in the interdependency matrix symbolizes a dependency between two parameters. If the interdependency matrix had been quadratic and diagonal, the crushing process would have been easy to analyse. In that case one input parameter would only affect one single output parameter. The process would have been easy to tune if, for example, speed had been the only parameter affecting capacity.

A process with a quadratic and triangular interdependency matrix would have been possible to tune by adjusting the input process parameters in correct order. In the case of crushing with existing crusher equipment, such as jaw and cone crushers, the interdependency matrix will be different from triangular. This is the fact behind the complexity of the crushing process. As an example it can be seen from Eq. (1) that the product size distribution is affected by all the independent parameters.

1.5.3 CRUSHER OPERATION

Owing to variations in the rock material, such as type of mineral, grain size, distribution of cracks etc., quality problems often occur.

Process control is desirable for maintaining high product quality, but today there are no systems available for this purpose owing to the absence of on-line detectors for product size distribution and shape. Another drawback is that very few models describing crusher characteristics are available.

A proposed system for closed loop process control is illustrated in Figure 6. To achieve closed loop process control, development of both detectors and crusher models is needed. Without detectors the system will be of the open loop type and thus very sensitive to feed variations and wear of the crusher chamber.

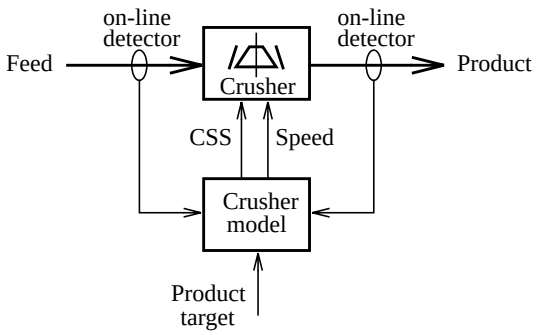

Figure 6. Possible system for process control of a single crushing stage. On-line detectors could be of the optical, acoustic or microwave type. Control signals from the crusher model are closed side setting (CSS) and eccentric speed.

In every crushing stage an undesirable amount of fine material is produced. The definition of fines varies, but a common definition is particles with a size of less than 2 mm. In some geographical regions the disposal of fines can be difficult. Therefore, it is of great interest to the ballast producing industry to reduce the production of fines, while still preserving the overall reduction ratio.

2 SCIENTIFIC APPROACH

This work was carried out at the Machine Element Group, Machine and Vehicle Design, Chalmers University of Technology. The focus of research within the group is on machine components and machines. The main activity is the systematic search for new knowledge concerning the principles of operation, characteristic behaviour and performance of the objects studied. It is believed that significant improvements in machine design can be achieved by fundamental understanding of the component or machine.

The research is problem oriented. This means that the problem itself is in focus and not the method or tools to solve it. The different steps in the problem oriented research method put into practice by the Machine Element Group are shown in Figure 7. The problem oriented research method is thoroughly described by Hultén [22].

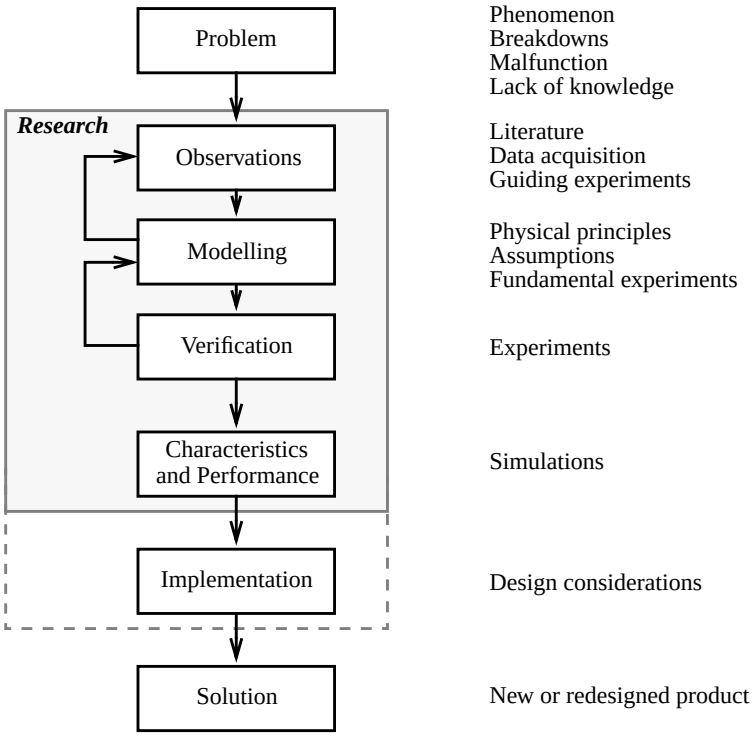

Figure 7. Structure of a problem oriented research process.

Research is defined as the activities undertaken to create new knowledge, which in turn is used to find a solution to the original problem.

Most research projects start with a problem. The character of the problem can be very different. Machines or components can reveal unexplained breakdowns or there are malfunctions. Unexpected phenomena might occur. Sometimes there is a lack of knowledge which originates from a need of increasing the performance of the object.

The first step in the research process is to identify a knowledge gap. Different kinds of observations are used for this purpose. Literature reviews are used to outline the current status of the knowledge base related to the problem. Data acquisition or guiding experiments can be performed in order to clarify the nature of the problem. When the knowledge gap is identified the objectives of the research project can be formulated.

Modelling is probably the most central part of the research process. The aim of modelling is to describe the phenomenon in mathematical terms. Already known physical effects are normally used when the models are formed.

Very often, the phenomenon is complex in nature. If the complete behaviour, including all possible aspects, is to be described, the mathematical model would be large and complex and thus difficult to use in simulations. In order to make the model possible to handle simplifications are needed. Assumptions and simplifications should be done on such a level that no restrictions are obtained at the level where the problem is formulated. Which assumptions and simplifications that should be made depend directly on the degree of explanation or resolution required of the final model.

The model structure can be described with a theory tree, see Figure 8. The theory tree is a hierarchical structure of submodels, which together form the hypothesis. The top level of the tree corresponds to the final model describing the problem. The different sub levels correspond to models which are often based on accepted theories taken from a common knowledge base.

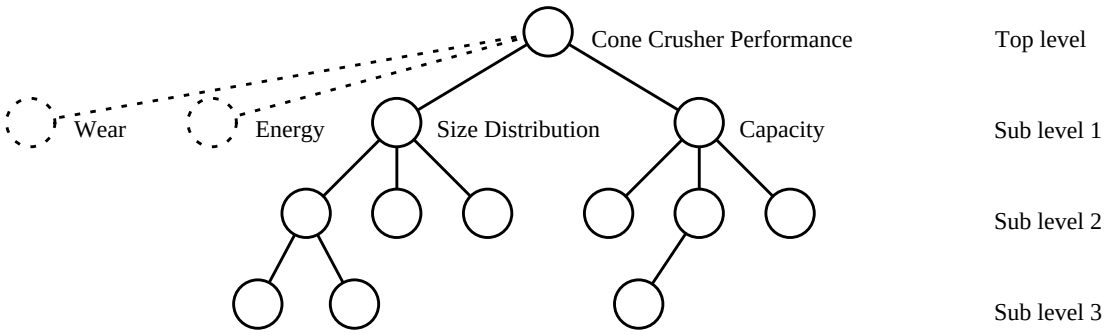

Figure 8. Theory tree.

If a phenomenon cannot be explained by already existing theories, fundamental experiments can be performed to obtain relations between different parameters. Typically, constitutive relationships are found in this way.

Verifications are carried out by experiments in order to verify the accuracy of the final model. The requirements set on the level of agreement differ depending on the aim of the model. To achieve a high qualitative correlation is often more important than to achieve quantitative agreement. If the verification fails, the model has to be improved, and in some cases new observations are needed.

Once a verified model is achieved, simulations can be carried out in order to obtain information about the characteristics and performance of the object studied. Through the physical effects used in the model, fundamental understanding is achieved. Compared to full-scale testing, mathematical simulations are usually far more cost effective. From the simulations, conclusions can be drawn concerning important effects and to which degree performance can be improved.

The new knowledge gained can be formulated in so-called design considerations. These considerations can be implemented by redesigning the original product or in a completely new design. Properly done the new product is a solution to the original problem.

3 OBJECTIVES

The overall purpose of this work is to achieve a fundamental understanding of how a cone crusher works from a size reduction point of view.

The objective of this thesis is to develop a theoretical model, which can be used to predict product size distributions and capacities from cone crushers. An important property of the process model is that it must be closely physically defined. Prediction of the performance of a cone crusher already at the design stage would enable improvements without full-scale testing. Crushers already existing in crushing plants can be investigated and the best operating parameters chosen.

Crushing is quite a complex process and the results are affected by both machine properties and rock properties. Therefore, machine design and operating conditions, together with the breakage characteristics of the rock material, should be taken into consideration.

Prediction of energy consumption and power requirement is not an objective of this work, as the operating principle of cone crushers is form conditioned. Energy consumption is considered to be a secondary effect of the size distribution process. Liner wear prediction is not an objective of work.

4 LITERATURE REVIEW

Historically, the process of size reduction has been studied in terms of the energy consumed during the operation of a comminution plant (Lynch [27]). This was a logical starting point because size reduction is responsible for a large proportion of the costs of ore treatment and the energy consumed is the major cost in size reduction. This basis of investigation was influenced more by the economics of the operation than by any other factor.

Relatively few models describing the size reduction process occurring in cone crushers have been presented. Bond's model [3], *Third Theory of Comminution,* presented in the early fifties is still frequently used today by manufacturers when selecting crusher equipment. The success of the model is probably explained by its ease of use and not by the quality of the predicted results. Before Bond presented his model, both Rittinger [30] and Kick [23] had worked with similar types of approach. The theories of Rittinger, Kick and Bond are described in details in *Paper A.*

For single fracture of a brittle solid, the distribution function for fragment size after fracture has been derived by Gilvarry [19]. The physical point of departure is the Griffith theory of brittle fracture [20]. The derivation is based on a closely defined physical model and deduced by the laws of probability. Single fracture of a brittle solid is defined as fracture by an external stress system, which is instantly applied and permanently removed when the first Griffith flaws begin to propagate. Subsequent flaws are activated by stress waves produced by propagation of prior ones. Comminution of a specimen by repeated fracture of specimens is excluded by the definition, since there is no assurance that the flaw distributions in the fragments exposed to the repeated breakage are the same as in the original specimen.

Rosin and Rammler [32] suggested an empirical equation describing the size distribution after breakage. Broadbent and Callcott [7][8] suggested a modification of the Rosin-Rammler equation for use in their investigations of coal breakage processes. The distributions given by Rosin-Rammler and Broadbent-Callcott are examples of some well-known and frequently used size distribution functions. During the last three decades a number of both analytical and empirical functions have been suggested by different authors. The mathematical form of the functions vary from simple to rather complex. Klimpel and Austin [24] derived an expression

in which they tried to link physical properties of the particles to the breakage function. Barnard and Bull [1] determined an empirical breakage function for the cumulative size distribution by performing drop-shatter tests with brown-coal.

Drop weight tests have been used by several authors. Examples of such work have been carried out by Rose [31] and Briggs [5].

Models describing interparticle breakage behaviour are relatively rare. Fewer tests have been conducted and reported with particle beds than with single particles. Prasher [29] concludes that this fact represents a research gap, since most industrial comminution involves beds, and single-particle tests cannot adequately represent the interaction of particles with different size, shape and orientation. Buss *et al.* [9] worked with the aspects of energy utilization in particle beds. Liu and Schönert [26] concluded that it should be possible to model closed circuit comminution with high pressure roller mills originating from models describing interparticle breakage. The problem with roller mills is in a way similar to cone crushers but there are also great differences. In a roller mill the material is only subjected to one single crushing event, in contrast to repetitive crushing in cone crushers. Interparticle breakage behaviour was modelled from an energy point of view. Size reduction in a cone crusher is form conditioned. Therefore energy is considered to be a secondary effect, i.e. instead of energy input there is energy consumption. Further, Schönert [33] has shown that the probability of a particle breaking depends upon the number of forces acting on it.

The well-known flow model developed by Gauldie [17][18] is only capable of predicting crusher capacity and does not embrace any ideas concerning the size reduction process. Gauldie's model has been used by several authors for prediction of the throughput from crushers [10][14]. The model has a serious weakness since it lacks a genuine constitutive law coupling size distribution to bulk density.

Empirical models, such as the one of Whiten [34][35], provide excellent guides for operational purposes but these models are insufficient for describing the going on size reduction and flow mechanisms in the crusher. These types of model cannot be used for design purposes.

Bearman [2] presented mathematical relationships which are capable of predicting energy and eighty per cent passing size of product based on identified controlling factors. These factors were certain rock strength parameters and discharge setting. Especially good predictions were achieved for the rock strength parameter fracture toughness. This is a strong indication that tensile failure is the dominating breaking mechanism in both jaw and cone crushers.

Crusher models which are based on laws of mechanics are very rare. Briggs [5] proposed a model based on equations of motion, but which was only capable of treating single particle breakage.

A large number of authors have worked with quality aspects of aggregate production (Eloranta [10], Heikkilä [21], Kojovic [25]). As long as no fundamental model has been accepted describing the crushing mechanisms in cone crushers, the conclusions are sometimes contradicting and may be dependent on the specific application.

5 MODEL DEVELOPMENT

The overall model for predicting cone crusher performance presented in this thesis has successively been developed in the following four parts:

- Size reduction process modelling
- Characterization of rock material breakage behaviour
- Flow modelling
- Interaction between flow and size reduction

Process modelling comprises identification of the comminution principle utilized together with the basic operating principle of cone crushers (*Paper A*). The overall size reduction process is modelled as a series of repeated crushing events. Form conditioned crushing tests are performed to characterize the fragmentation behaviour of different rock materials (*Paper B*). Equations of motion are used to describe the flow of material in the crushing chamber (*Paper D*). A geometry module capable of handling arbitrary chamber geometries delivers geometrical data to the flow model. To guarantee that mass continuity is preserved and that no other requirements are violated the interaction between material flow and size reduction is given some extra attention (*Paper E*).

5.1 STRUCTURE OF CRUSHER ANALYSIS

In Figure 9 a structure for analysis of a cone crusher is shown (*Paper D*). To calculate the product size distribution of the output from a cone crusher according to the suggested structure, two main calculation models are needed. These models are:

- Size reduction model
- Flow model

The size reduction model predicts the size distribution after compressing the rock material. Every single reduction step is described by a *selection* and a *breakage* function. The flow model is important since it describes how the rock material moves down through the crusher chamber. Thereby the flow model provides input to the size reduction model which is used to determine the values of the selection and breakage functions. Two models for flow and size reduction respectively have been presented earlier (*Papers A, B, C, D and E*). The interaction between these two models is quite complex and intricate, as the overall size reduction in a cone crusher is a result of a repeated consecutive comminution process.

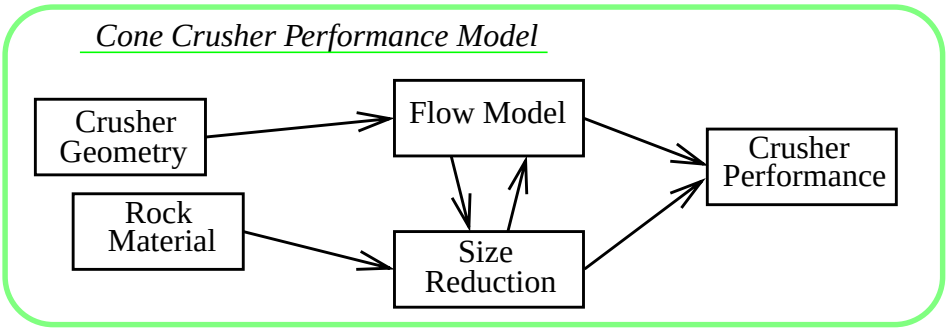

Figure 9. Structure of the crusher performance model.

The flow and size reduction models will be closely tied together as the input to the size reduction model will depend on the result of the flow model. In turn, the flow model will depend on the size distribution, as there will be several repeated consecutive reduction steps.

Further information needed to carry out the calculations is:

- Fragmentation behaviour
- Crusher geometry
- Density model (constitutive relation between size distribution and density)

The fragmentation behaviour or the breakage characteristics are achieved from form conditioned compressive bed tests where an aggregate of particles is comminuted under controlled conditions (*Paper B*). Any existing and non-existing profile design must be able to be analysed by the crusher geometry module. Mantle and concave geometries together with other important crusher parameters are given as input to a geometry module (*Paper D*). This module provides the data needed for the flow model. A constitutive relationship which relates size distribution to uncompressed bulk density is needed as the density varies with particle size distribution (*Paper D*).

5.2 MODULAR APPROACH

Based on the structure in Figure 9, a calculation method has been developed which has been implemented in a computer program. A modular approach is suitable and natural according to the structure of the calculation method. Each module is self sustained and can be upgraded or replaced, if needed. The information flow follows the direction of the arrows in Figure 10.

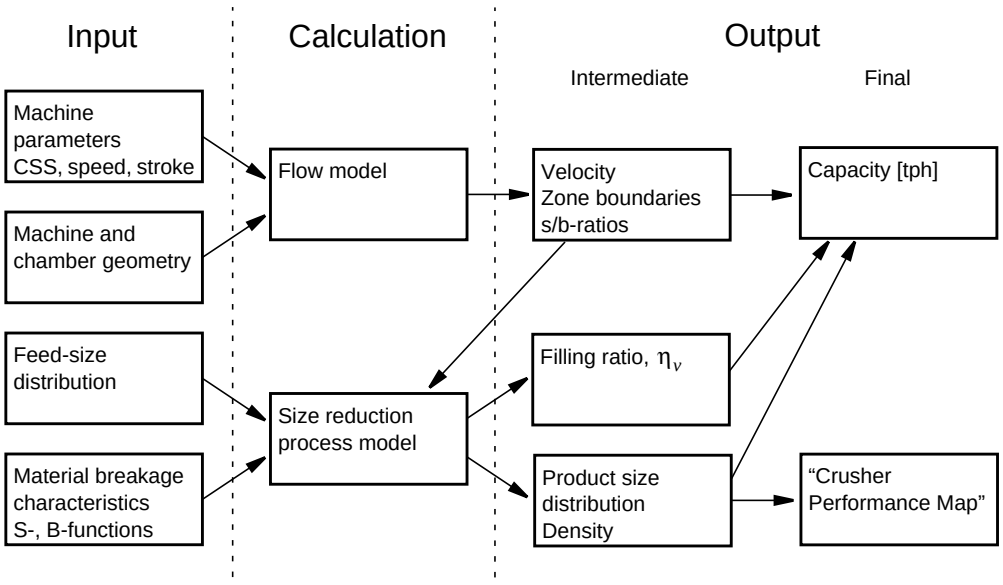

Figure 10. The calculation method has a modular structure. Every single module can be replaced if necessary.

Input to the calculation method are machine parameters such as closed side setting (CSS), speed, stroke, chamber geometry, feed size distribution and material breakage characteristics. Input is divided into four modules. Prediction of material flow and size reduction is performed in two separate modules. Output from the method are capacity and product size distribution. Zone boundaries and compression ratios (s/b-ratios) are calculated as intermediate results.

5.2.1 CRUSHER PERFORMANCE MAP

By combining the total capacity with the product size distribution for every eccentric speed one will achieve a set of curves corresponding to the net capacity for different product gradings. The final result achieved is called a *Crusher Performance Map* (*CPM*). The CPM can be multi-

dimensional and shows how the final product depends on variations in machine parameters for a given crushing chamber and feed. A Crusher Performance Map for a tentative cone crusher is shown in Figure 11 (Paper C). This particular CPM is two-dimensional as it was calculated for only one value of the CSS. It can be seen that the eccentric speed has a great influence on the final product i.e. size distribution and net capacities of different product gradings are affected by the eccentric speed.

The crusher performance map describes the combined response from the interaction between crusher and rock material. Only the total capacity is independent of material choice and thus valid for all rock materials. The map in the general case is multidimensional and has as many dimensions as there are machine parameters. In the case where eccentric speed and closed side setting are the varying parameters the crusher performance map will have three dimensions.

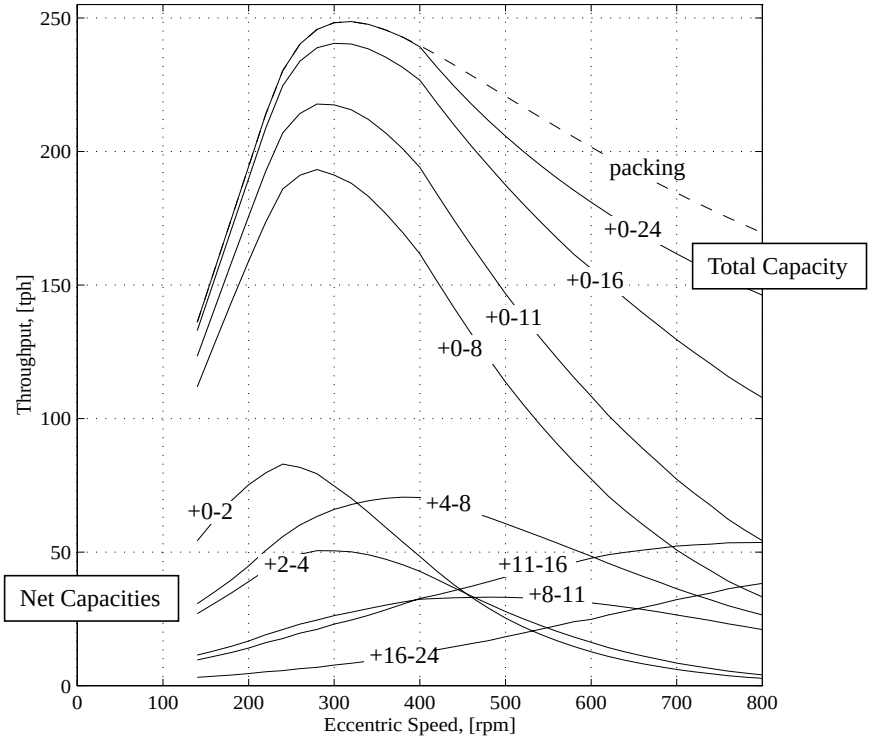

Figure 11. Crusher Performance Map for a tentative cone crusher showing the capacities for different product gradings. Only interparticle breakage is considered (Paper C).

From the crusher performance map it is obvious that total capacity and all net capacities varies quite substantially with eccentric speed. For eccentric speed higher than 400 rpm packing occurs if the feed to the crusher is not restricted. Net capacities for different product gradings does not have maxima at the same eccentric speed. This fact makes optimization very interesting and challenging. It is up to the aggregate producer to formulate criteria to which the optimal eccentric speed can be chosen.

6 NOMINAL GEOMETRY

Before any simulations can be carried out, the nominal crusher chamber geometry has to be encoded numerically. For this reason an input module for geometry was designed (*Paper D*). By means of the generally designed input module, every possible chamber geometry can be treated. The calculations in the flow model are therefore based on true geometry. Every existing chamber geometry, independent of brand and model, can be described with a set of nodes which are connected with arcs or straight lines. If desired, any arbitrary continuous function can be used to describe the profile of the chamber geometry between two given nodes.

The nominal geometry for a Svedala Hydrocone crusher is shown in Figure 12. Already at this stage it is possible to calculate a set of nominal parameters that characterize the crusher chamber. Nominal stroke and bed thickness are determined at every point of a cross-section of the chamber. The ratio between stroke and bed thickness is called the *nominal compression ratio* and is denoted $(s/b)_{nom}$. This parameter is central for later predictions of size reduction.

The horizontal cross-sectional area is calculated at all vertical levels. The minimum of the cross-sectional area defines the so-called *choke level* of the crusher chamber. The location of the choke level is important since it will control the different types of breakage modes in the crushing chamber.

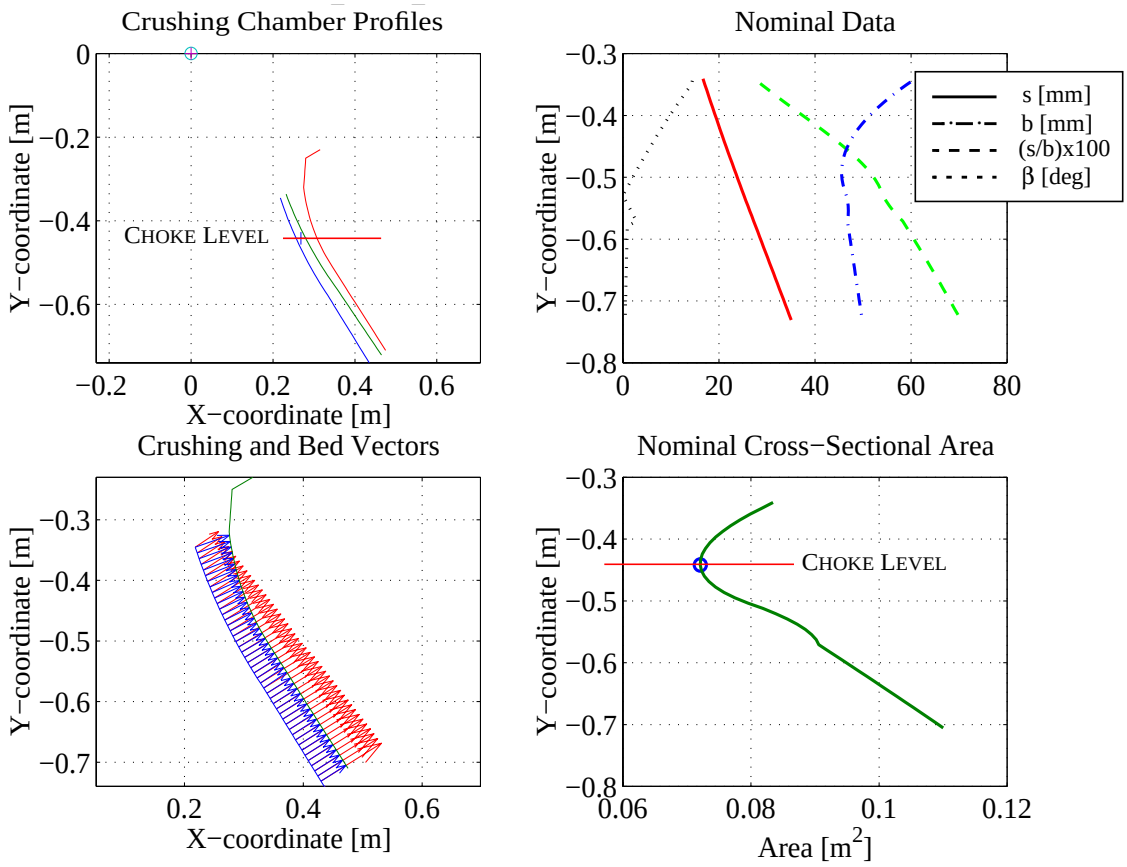

Figure 12. Nominal geometry for a Svedala Hydrocone crusher (Paper D). β *is the angle between the crushing and bed vectors.*

7 SIZE REDUCTION PROCESS MODEL

In a cone crusher the incoming feed material is transformed to product by a repeated comminution process. The number of reduction steps varies between different crushers, but it has been shown that it can be ten or more (*Paper D*). An analytical model describing the process should therefore include all these reduction steps.

In Figure 13, a model is presented using two basic mechanisms for describing each single reduction cycle, viz. selection and breakage (*Paper A*). The product from one crushing event is the feed to the following one. The size reduction occurring in every single crushing event is described by a selection and a breakage function. It is believed that these two mechanisms can describe all aspects of importance of the breakage behaviour.

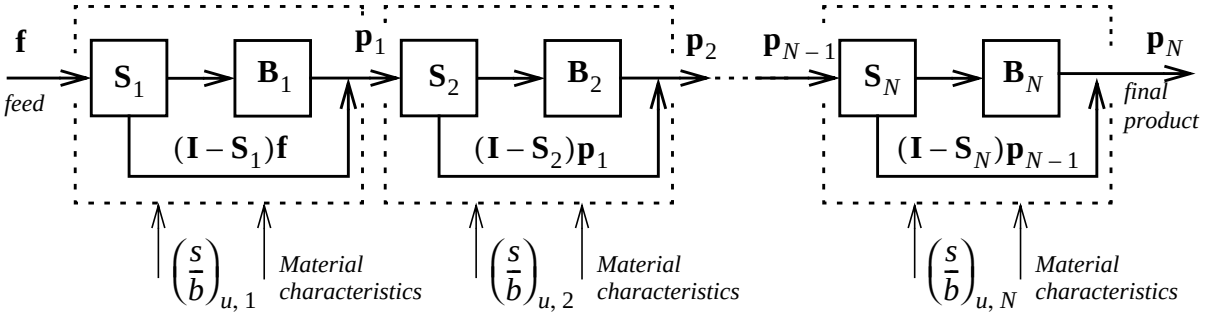

Figure 13. Process model of a cyclically operating crusher with N consecutive crushing events. The utilized compression ratio $(s/b)_u$ is determined from the location of each crushing event, crusher dynamics and rock material density (Paper E). S=selection, B=breakage.

Selection S corresponds to the probability of a particle being broken. *Breakage B* reflects the way a particle is broken, i.e. the size distribution of the daughter fragments. By introducing matrix algebra, every single reduction step can then be described as

$$\mathbf{p}_i = [\mathbf{B}_i\mathbf{S}_i + (\mathbf{I} - \mathbf{S}_i)]\mathbf{p}_{i-1} \qquad (2)$$

where $\mathbf{p}_i$ represents the product from and $\mathbf{p}_{i-1}$ the feed to step i. Furthermore, $\mathbf{B}_i$ and $\mathbf{S}_i$ are matrix operators corresponding to breakage and selection, respectively. The total number of crushing events occurring within the modelled crusher is denoted N. The value of the elements in the breakage and selection matrices $\mathbf{B}_i$ and $\mathbf{S}_i$ will vary depending on the location in the crusher chamber. The dimensionless machine parameter $(s/b)_u$ is called the compression ratio. This parameter describes how much the rock material is compressed at a certain location in crushing event i. The compression ratio is therefore used to determine the values of the elements in $\mathbf{B}_i$ and $\mathbf{S}_i$. The value of $(s/b)_u$ is obviously a key parameter for size reduction and should therefore be delivered by the flow model.

Two different main types of breakage can occur in a cone crusher. The different kinds of breakage are called breakage modes. The two breakage modes considered are interparticle and single particle breakage. The breakage modes are not mutually exclusive, but can occur simultaneously in a breakage zone depending on the surrounding conditions.

By introducing a mode matrix $\mathbf{M}_i$ to Eq. (2), a general expression including both types of breakage is achieved (*Paper A*). A crushing event where both interparticle and single breakage occur is shown in Figure 14. The corresponding mathematical description is given in Eq. (3). The mode matrices are diagonal by definition, and the only values the elements can take are one or zero. The sum of the mode matrices is identical with the identity matrix $\mathbf{I}$, in which the elements are one in the main diagonal and zero in every other position.

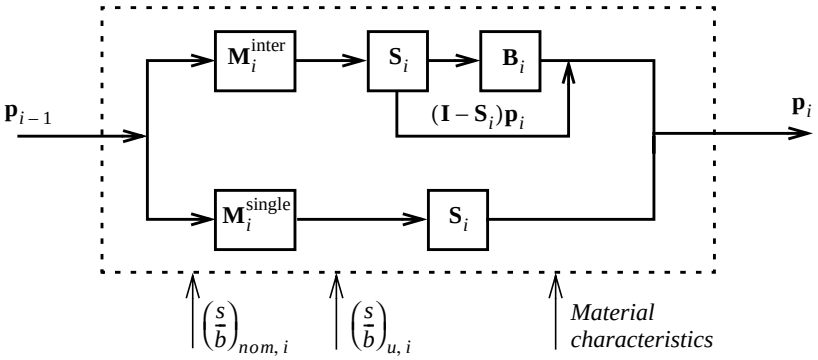

Figure 14. A single crushing event comprising both interparticle and single particle breakage. Depending on particle size and the location in the crushing chamber a particle will either be crushed in the interparticle or the single particle breakage mode.

$$\mathbf{p}_i = [[\mathbf{B}_i^{\text{inter}}\mathbf{S}_i + (\mathbf{I}-\mathbf{S}_i)]\mathbf{M}_i^{\text{inter}} + \mathbf{B}_i^{\text{single}}\mathbf{M}_i^{\text{single}}]\mathbf{p}_{i-1} \quad (3)$$

$$\mathbf{M}_i^{\text{inter}} + \mathbf{M}_i^{\text{single}} = \mathbf{I} \quad (4)$$

The conditions that control and activate the different breakage modes are the degree of confinement and the local closed side setting (*Paper E*). It is assumed that interparticle breakage occurs above the choke level where confined particle beds are obtained. Furthermore, single particle breakage occurs when a particle is nipped between mantle and concave. It is assumed that this is the only breakage mode obtainable below the choke level.

8 ROCK FRAGMENTATION CHARACTERISTICS

Jaw, cone and gyratory crushers all utilize form-conditioned compression to achieve size reduction. For this reason geometry controlled (form conditioned) compression crushing tests are performed to achieve the breakage characteristics of the rock material (*Papers B and E*). The breakage behaviour is described mathematically by a selection and a breakage function. From the form conditioned compression tests, the breakage behaviour is obtained as a primary effect of the compression ratio. Force and energy are secondary but important parameters and can be obtained if desired.

8.1 BREAKAGE BEHAVIOUR ASSUMPTIONS

The two functions S and B constitute a description of the breakage behaviour for the rock material of interest. Some crucial assumptions are needed to make it possible to obtain S and B by laboratory tests.

The value of the selection function S varies both with the compression ratio and with the size distribution of the material which is to be crushed. The value of S varies with the size distribution width but is independent of particle size within a given size distribution. The particle size distribution is characterized by its width or spread and is assumed to be reflected by a normalized standard deviation $\sigma_{\aleph}$ of the distribution.

The breakage behaviour is described with a breakage function B. The breakage function is a cumulative function and the value of B describes the relative amount (by mass) of particles passing a given relative size. For a given original particle size, the breakage behaviour is

assumed only to be dependent on the compression ratio. This means that a large particle gives rise to a size distribution of the daughter fragments similar to a small particle, if the size scale is normalized by the original size.

8.2 SIZE DISTRIBUTION WIDTH

It is desirable to describe a particle size distribution with a single number. Here, the size distribution is assumed to be characterized by the normalized standard deviation $\sigma_{\aleph}$ of the frequency function f corresponding to the size distribution (*Paper E*). The normalized standard deviation is achieved by dividing the standard deviation σ by the mean value $\bar{x}$ of the distribution

$$\sigma_{\aleph} = \frac{\sigma}{\bar{x}} \tag{5}$$

where σ and $\bar{x}$ are defined by

$$\sigma^2 = \frac{1}{N-1}\sum_{i=1}^{n} f_i(x_i - \bar{x})^2 \qquad \bar{x} = \frac{1}{N}\sum_{i=1}^{n} f_i x_i \qquad N = \sum_{i=1}^{n} f_i \tag{6}$$

The advantage of using the normalized standard deviation as a measure of the spread of the size distribution is that this number will be independent of particle size. Further, the normalized standard deviation will always take values in the interval zero to one.

8.3 COMPRESSION CRUSHING TESTS

Knowledge about the appearance of the S and B functions is needed before any simulations can be carried out using the size reduction model. To quantify the S and B functions, laboratory-scale compression crushing tests were performed (*Paper E*). In the tests, the rock material is crushed in a steel cylinder. The equipment is designed to imitate the conditions, in which a volume of material is compressed in a real crushing chamber (*Paper B* and [12]). The laboratory test corresponds to the compressing part of the machine cycle when the liners move towards each other. The material is then locked between the chamber walls and can only deform elastically, plastically and/or break into smaller particles. The compression is form conditioned. For the rock materials of interest, brittle fracture is the only fracture mechanism of importance. At normal operating conditions, the maximum radial velocity of the mantle relative to the concave is below 0.5 m/s. It is assumed that the breakage and selection appearance are independent of the strain rate at this level.

For laboratory compression tests, the normalized compression ratio is denoted $s_{\aleph}$. The same variable is called the utilized compression ratio $(s/b)_u$ if it is achieved from calculations originating from the crusher model. The numerical values have the same meaning regarding these two variables.

The tests were performed in six different series, each with a constant compression ratio $s_{\aleph}$. The material chosen for the tests was gneiss taken from a quarry in Dalby in southern Sweden where Svedala has a test-plant facility. The same material was used in the simulations and the full-scale tests. The first test in each series were done on a mono-sized aggregate of fraction +16-19 mm. The remaining tests were done on the material originating from the preceding tests. After every compression test the material was sieved. The resulting size distributions from each test are shown in Figure 15.

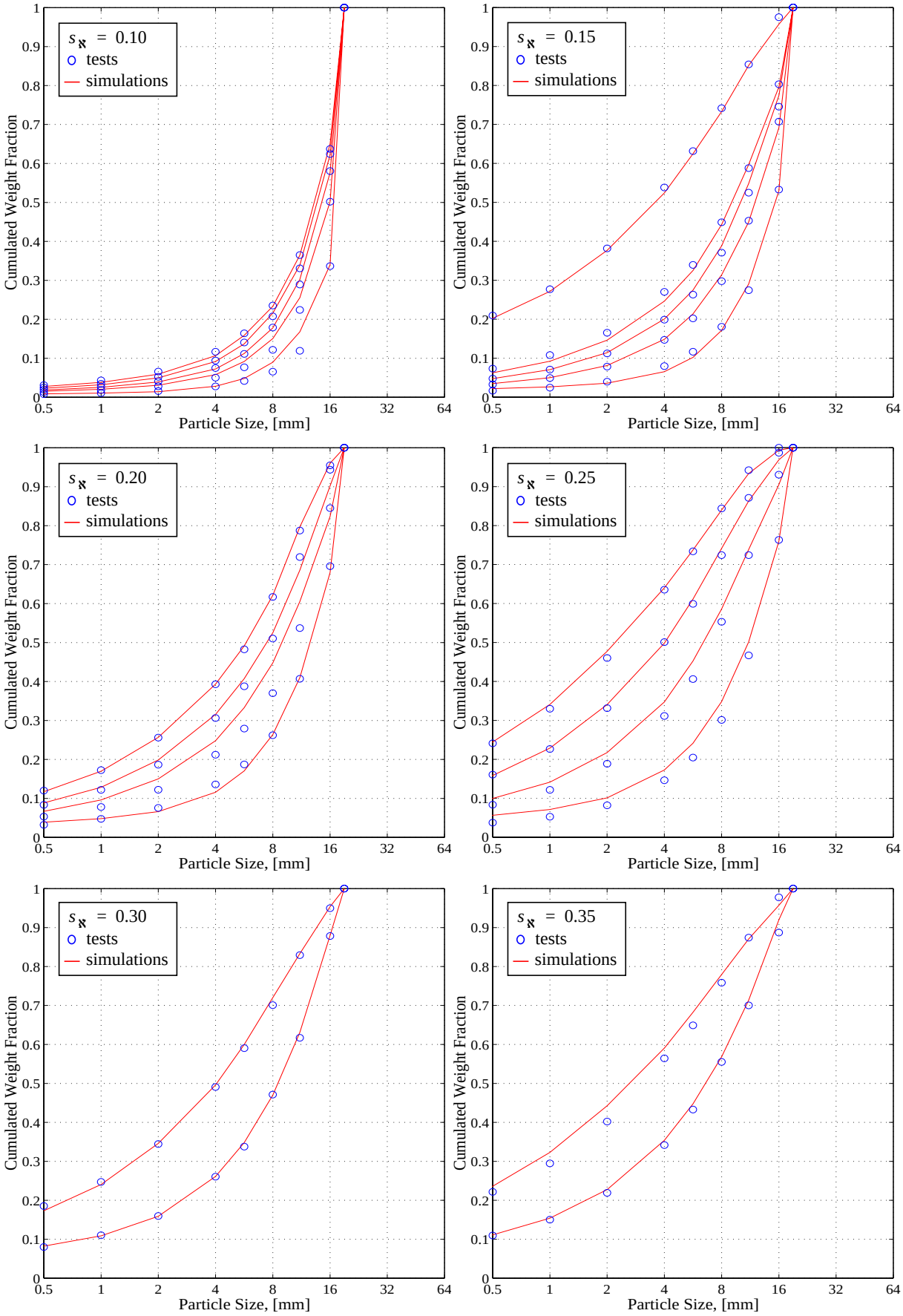

Figure 15. Test and simulated results from the six series of consecutive compression crushing tests.

8.4 SELECTION

The value of selection is obtained directly from the compression tests. For the first test in each series with the narrow size distribution, defined by $+x_1$-x_0 (+16-19 mm), the value of S is simply obtained as the weight fraction passing size x_1 (16 mm). For the following tests the value of S is achieved as

$$S_i = \frac{W_i^{x_1} - W_{i-1}^{x_1}}{1 - W_{i-1}^{x_1}} \tag{7}$$

where $W_i^{x_1}$ is the weight fraction passing size x_1 after test i and S_{i-1} is the value of the selection function from the preceding test. The achieved values of S are plotted in Figure 16a against the compression ratio. It is clear that the breakage probability S varies both with the compression ratio $s_\aleph$ and with the feed size distribution $\sigma_\aleph$. The value of S increases with increasing $s_\aleph$ which is an obvious and natural behaviour. The size distribution width influences the value of S, so that for short fractions higher values of the breakage probability are obtained compared to wide fractions.

A two-variable selection function $S(s_\aleph, \sigma_\aleph)$ given in Eq. (8) can satisfactorily describe the breakage probability (*Paper E*). The appearance of the selection function achieved after fitting Eq. (8) to experimental data is shown in Figure 16. The good fit with the experiments confirms the assumption about the behaviour of the selection function.

$$\begin{aligned} S(s_\aleph, \sigma_\aleph) = {} & a_1 s_\aleph^2 \sigma_\aleph^2 + a_2 s_\aleph^2 \sigma_\aleph + a_3 s_\aleph^2 \\ & + a_4 s_\aleph \sigma_\aleph^2 + a_5 s_\aleph \sigma_\aleph + a_6 s_\aleph + a_7 \sigma_\aleph^2 + a_8 \sigma_\aleph + a_9 \end{aligned} \tag{8}$$

The values of the fitted constants a_i for the tested material are

$a_1 = -17.20202$	$a_2 = 1.64983$	$a_3 = -4.61729$
$a_4 = 6.26490$	$a_5 = 1.41795$	$a_6 = 4.21650$
$a_7 = -0.025766$	$a_8 = -1.22568$	$a_9 = 0.055819$

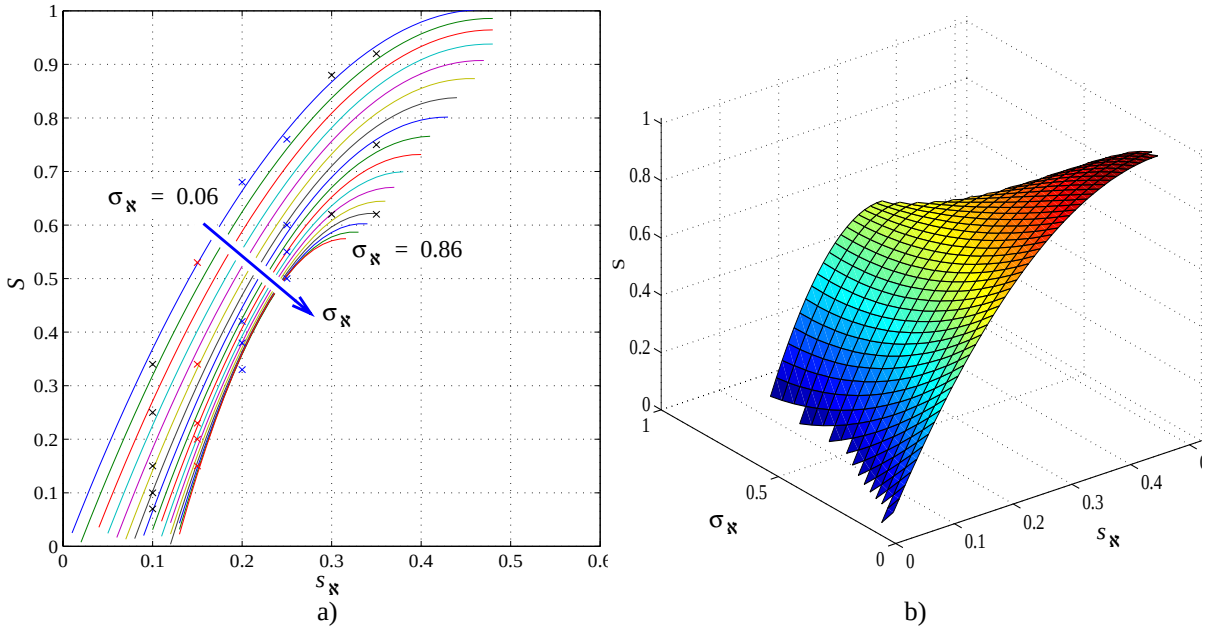

Figure 16. a) Two-variable selection function fitted to experimental data.
b) In 3D the function appears as a surface in space.

8.5 BREAKAGE

The breakage behaviour is assumed only to be dependent of the compression ratio. Therefore, to calibrate a breakage function it is sufficient to use the result from the first test in each series shown in Figure 15. Normalized size distributions resulting from the compression tests with different $s_{\aleph}$-ratios are shown in Figure 17. These breakage functions are obtained by normalizing the size distribution curve below size x_1 (16 mm) with the value of S in the corresponding case.

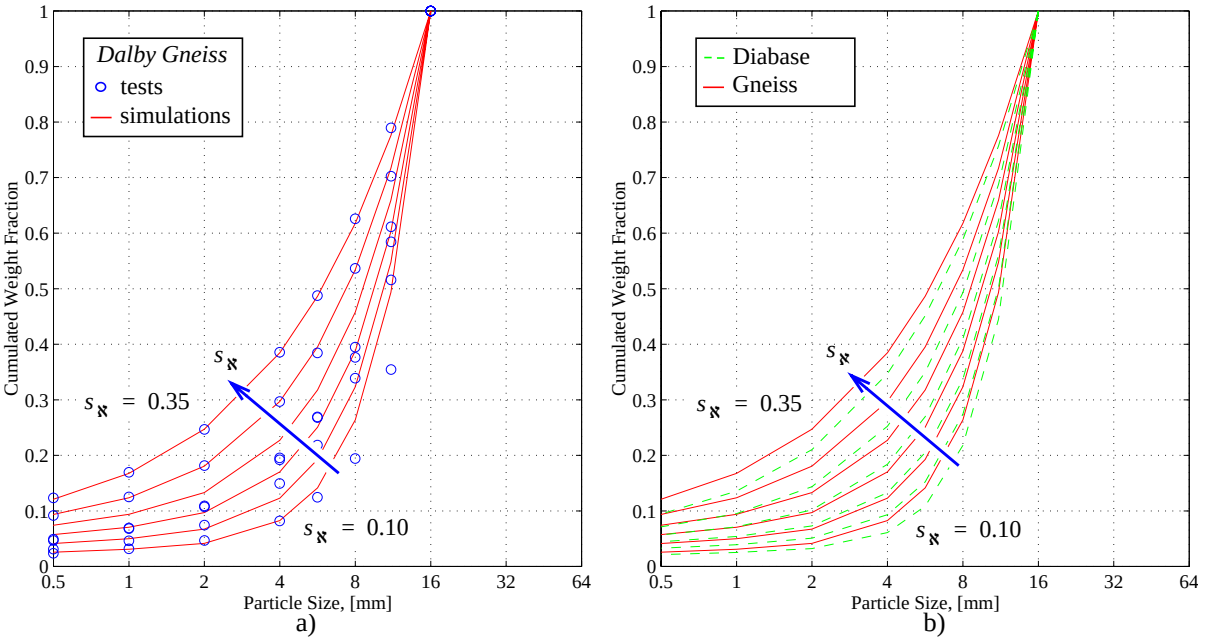

Figure 17. a) Normalized breakage behaviour of the tested gneiss material (Paper E).
b) Comparison of the breakage behaviour for diabase (Paper B) and gneiss (Paper E).

It is obvious that the overall reduction increases when the $s_{\aleph}$-ratio increases. A function given in Eq. (9) with $s_{\aleph}$ as parameter and four constants can be fitted to the experimental data (*Papers B and E*). Here $x_{\aleph}$ is a particle size relative to the initial particle size x_0. The particle size x_s is defined in Eq. (10) in which x_{min} is a small reference particle size (x_{min} = 0.008 mm).

$$B(x_{\aleph}, s_{\aleph}) = (1 - (\alpha_3 + \alpha_4 s_{\aleph}))x_s^{\alpha_1 + \alpha_2 s_{\aleph}} + (\alpha_3 + \alpha_4 s_{\aleph})x_s \qquad (9)$$

$$x_{\aleph} = \frac{\log_2(x/x_{min})}{\log_2(x_0/x_{min})} \qquad (10)$$

After fitting Eq. (9) to the data for gneiss in Figure 17 the numerical values of the constants are (*Paper E*)

α_1 = 18.9539 α_2 = –36.2309 α_3 = –0.0095 α_4 = 0.5657

For comparison data for diabase are also shown in Figure 17 (*Paper B*). It can be noted that the two different types of rock materials have a similar breakage behaviour. Though, for a given compression ratio, gneiss generates more fines than diabase.

Finally, the obtained selection and breakage functions were applied to each test in Figure 15. The simulated results are in good agreement with the tests, which confirms the overall breakage behaviour approach and assumptions. It is assumed that the obtained breakage behaviour can be used in the simulations of repeated size reductions in a cone crusher.

9 FLOW MODEL

The crushing process is modelled as a series of repeated crushing events. The flow model must therefore predict where and under which conditions (how) the material is compressed during each size reduction cycle. The overall size reduction process is described in Eq. (2). For a given rock material, the operators $\mathbf{S}_i$ and $\mathbf{B}_i$ depend on the dimensionless machine parameter $(s/b)_u$. The flow model should therefore predict the compression ratio at those points where a material volume is subjected to the crushing events (*Papers B and C*).

The flow model must be able to handle variations in both design and operational parameters. The design parameters are all the geometric parameters needed for describing different chamber profiles or crusher designs. For a given design or crusher, the operational parameters are closed side setting CSS, eccentric speed n and nominal stroke s_{nom}.

9.1 MATERIAL FLOW MECHANISMS

The flow model developed is based on equations of motion (*Paper D*). Three different mechanisms are assumed to describe the material flow, namely *sliding*, *free fall* and *squeezing*. Sliding occurs when a rock particle is in contact with the mantle and slides downwards. If the mantle accelerates away rapidly enough, the corresponding particle will fall freely. The free falling particle can catch up and impinge on the mantle surface. If so, the impact is modelled as fully plastic. If the mantle is still moving away from the concave, the particle will continue its motion by sliding.

The motion of particles relative to the mantle surface is assumed to cease and stop instantly when the particle is in contact with the mantle surface *and* when the mantle is moving towards the concave. This assumption implies inherently that bridging of particles occurs for the stated conditions. Bridging is a self-locking mechanism which forces the particle motion to stop relative to the mantle surface.

Once the particles have stopped moving, squeezing will start. During squeezing, particles will be compressed and thereby crushed. Fragmentation by brittle fracture will occur when the induced tensile stresses exceed a critical value. Particles which are smaller than the local closed side setting will be exposed to interparticle breakage. These particles will be in contact with both mantle and concave and thus they will be exposed to single particle breakage during squeezing.

Depending on the material transport mechanism, three different speed regions have been identified (*Paper D*). How the particle is transported in these three speed regions is shown in Figure 18. During squeezing the velocity of the particle is determined by the mantle motion. The velocity of the particle relative to the mantle surface will be zero. Shear stresses might occur depending on the chamber geometry.

At low speeds the motion of the particle is purely determined by sliding. Sliding will occur until the particle is nipped between the mantle and the concave. As long as the mantle surface is moving away from the concave, sliding will occur. This is defined as speed region I.

In speed region II the eccentric speed is high enough to accelerate the mantle surface away from the particle. The particle will then fall freely. At some point the particle will catch up with the mantle surface. If the mantle is still moving away from the concave the particle will continue its motion with sliding.

At high speeds the particle will be in free fall and impinge on the mantle at an eccentric angle greater than π. This is speed region III.

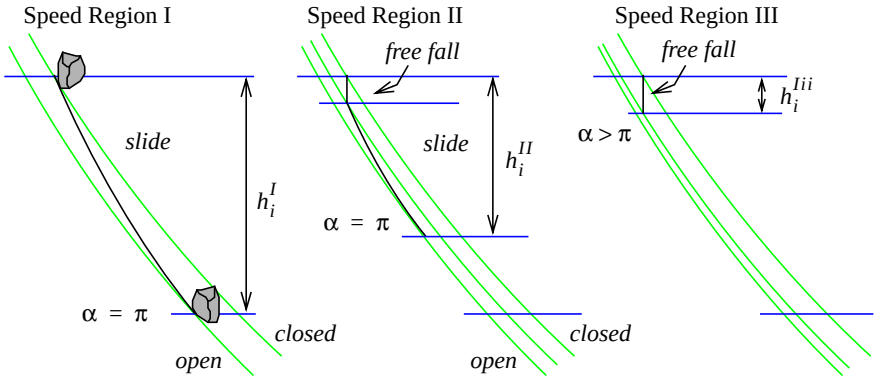

Figure 18. Three speed regions are defined depending on the active mechanism for material transport (Paper D).

Depending on the speed region the effective stroke that will be used for compression and crushing will vary. The effective stroke can be equal or less than the local nominal stroke. How the nominal stroke is utilized, depending on the transport mechanism, is shown in Figure 19. It is concluded that geometry controls the motion of the particle at low eccentric speeds while crusher dynamics controls the motion at higher speeds. In speed region I and II the local nominal stroke is fully utilized and therefore equal to the effective stroke. The effective stroke is less than the nominal one in speed region III.

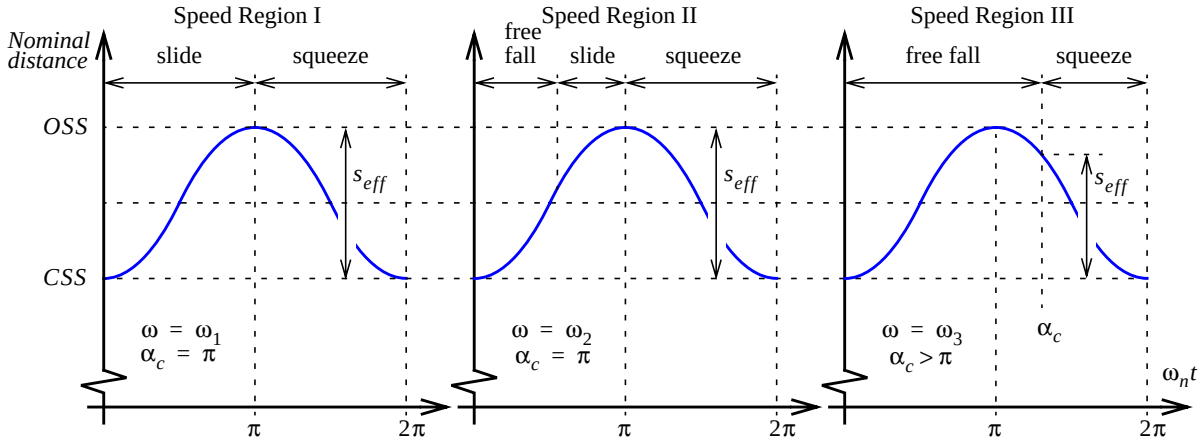

Figure 19. The effective stroke varies depending on the eccentric speed ($\omega_1 < \omega_2 < \omega_3$).

By performing repeated strokes it is possible to show how a particle is transported down through the crusher chamber. As the predominant flow mechanism is free fall, this simulation will give us the fastest possible way a particle can take. Examples of the resulting paths from repeated strokes are shown in Figure 20.

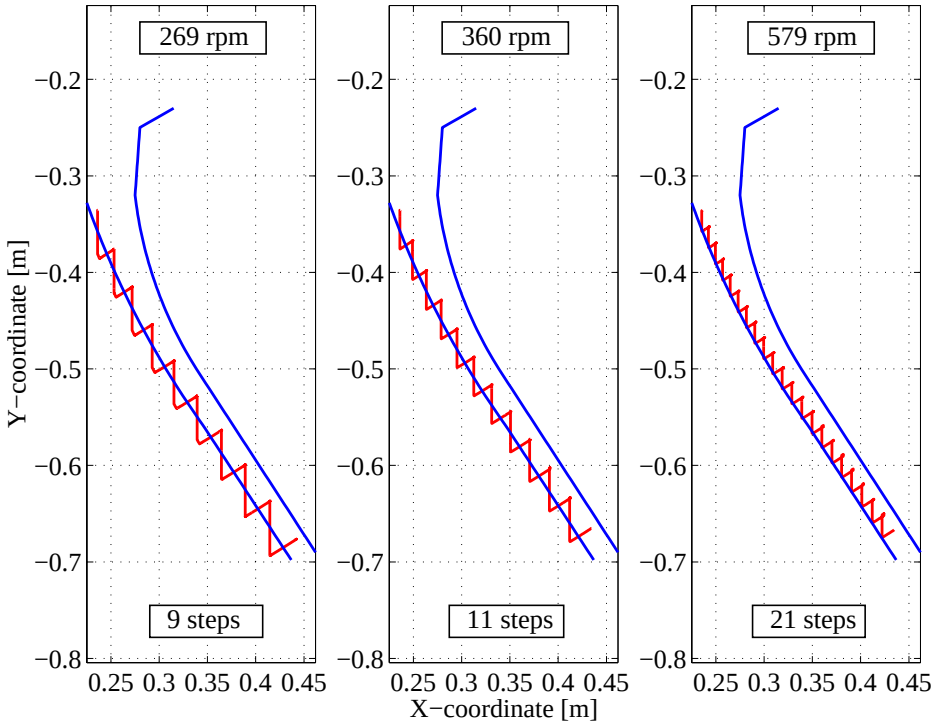

Figure 20. Repeated strokes show how a particle is transported through the crusher chamber. When the eccentric speed increases, the number of crushing zones increases. The mantle profile is shown in its neutral position (Paper D).

From the simulation the so-called crushing zones are defined. A crushing zone corresponds to a volume of material which is crushed when the eccentricity of the main shaft is turned one lap. The boundaries of a crushing zone are set by the mantle and concave surfaces together with lines perpendicular to the mantle surface. These lines intersect the starting and finishing points of the simulated path for each crushing step. When the locations in space and time are known for these zones, the geometry module will provide all geometrical data needed for the size reduction calculations.

9.2 VELOCITY DISTRIBUTIONS

Putting the flow mechanisms and other assumptions together will result in a velocity distribution which has the eccentric angle (or time) as independent parameter. The velocity distribution will depend on the eccentric speed. This will in turn reflect the active flow mechanisms. Some theoretical velocity distributions corresponding to different eccentric speeds is shown in Figure 21.

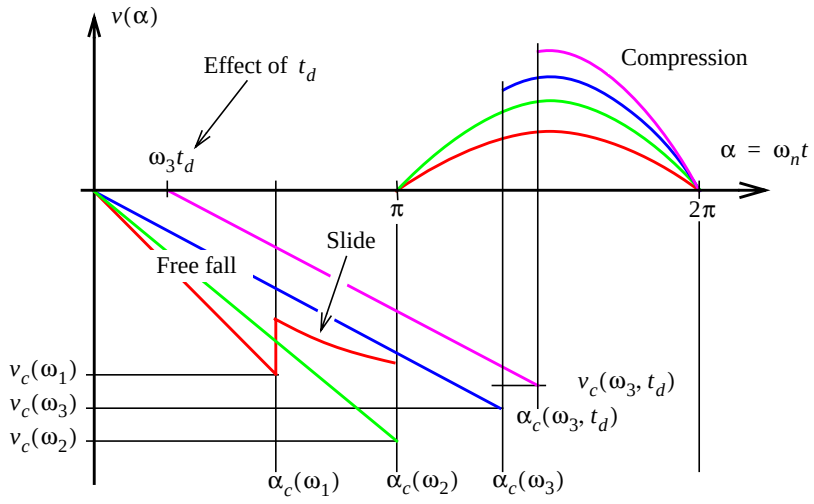

Figure 21. Velocity distributions as a function of eccentricity angle α*, with eccentric speed as parameter (*$\omega_1 < \omega_2 < \omega_3$*) (Paper D).*

Let us introduce a short time delay t_d. During this time period the particle does not move relative to the mantle surface. The time delay provides the possibility to handle feed material with varying moisture content.

9.3 CAPACITY

Once the velocities of all particles in a horizontal cross-section are known it is possible to calculate the capacity. In the simulations we will simulate a full crushing cycle of a particle which starts from rest at the choke-level. The choke-level is defined as the level where the area of a horizontal cross-section has its minimum. Then we will approximate the velocity field at the choke level with the velocity distribution of the particle. This simplification is not likely to give any serious impact since the total falling distance per cycle is quite small (less than 60 mm at low speeds).

The capacity is calculated by integrating the mass-flow field over a horizontal cross-section of the crushing chamber. In theory, the vertical level where the integration is carried out can be chosen arbitrarily. A natural choice is the level where the cross-sectional area has its minimum. For most crushers this level will be identified as the choke-point which controls the capacity of the crusher. A horizontal cross-section through the crushing chamber is shown in Figure 22.

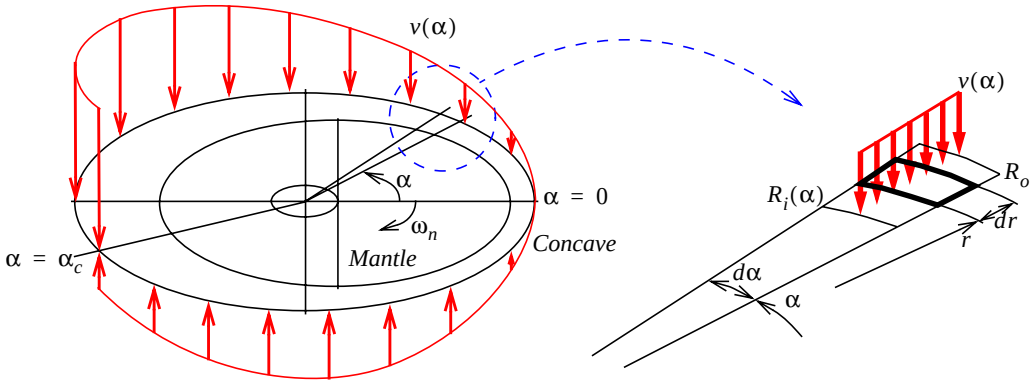

Figure 22. Horizontal cross-section of the crushing chamber (Paper D).

The mass flow in the downward direction will be

$$Q_{down} = \int_0^{\alpha_c} \int_{R_i(\alpha)}^{R_o} \rho v(\alpha) r dr d\alpha = \frac{1}{2} \int_0^{\alpha_c} \rho (R_o^2 - R_i^2(\alpha)) v(\alpha) d\alpha \quad (11)$$

$$R_{i,\,min} \le R_i \le R_{i,\,max} \quad (12)$$

The radius $R_i(\alpha)$ is the radius from which a particle with speed $v(\alpha)$ originates. The bulk density of the aggregate is denoted ρ.

In the upward direction we will have to divide the mass flow by two as particles in contact with the concave surface will have zero vertical velocity.

$$Q_{up} = \frac{1}{2} \int_{\alpha_c}^{2\pi} \int_{R_i(\alpha)}^{R_o} \rho v(\alpha) r dr d\alpha = \frac{1}{4} \int_{\alpha_c}^{2\pi} \rho (R_o^2 - R_i^2(\alpha)) v(\alpha) d\alpha \quad (13)$$

The overall capacity is then calculated as

$$Q = \eta_v (Q_{down} - Q_{up}) \quad (14)$$

We here introduce a volumetric filling ratio η_v. This parameter is equal or less than one depending on how well filling of the crushing zone is achieved.

So far, we have assumed that the velocity is equal for all points in the radial direction during the downward motion, see Figure 23. This is a first-order approximation. A more general approach would be to assume some distribution of the velocity in the radial direction.

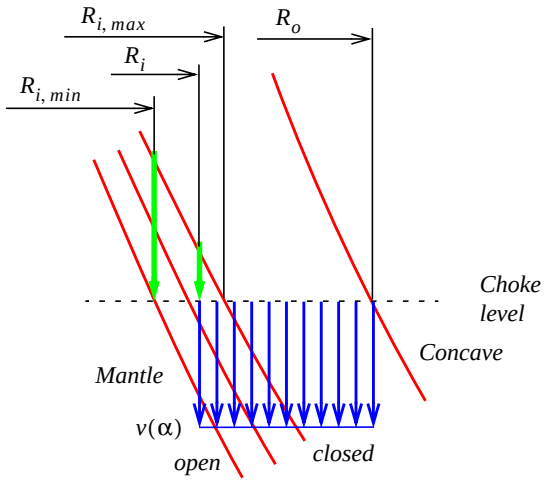

Figure 23. The assumed velocity distribution for a vertical cross-section (Paper D).

10 INTERACTION BETWEEN ROCK FLOW AND SIZE REDUCTION

The flow model predicts the locations and the effective compression ratios of the crushing zones. So far, no interaction between crusher and rock material has taken place with respect to size reduction.

The mathematical interaction between the flow and size reduction model comprises the problem to find a solution, which predicts the size distribution after every crushing step, and which also fulfils stated conditions (*Paper E*).

10.1 MASS CONTINUITY

Mass continuity must be preserved between all crushing zones and at any moment in time. The capacity in the downward direction Q_{down} can be achieved by multiplying the rotational speed n of the eccentricity by the specific mass flow m_i. The specific mass flow is equal to the bulk density of the aggregate ρ_i multiplied by the zone volume V_i. This is basically Gauldie's approach and is a slight approximation. To preserve continuity means that the value of the specific mass flow is constant for all zones. It has been found necessary to introduce a volumetric filling ratio $\eta_{v,i}$ (*Papers D and E*). The value of this parameter reflects to what extent an accessible zone volume is utilized.

$$Q_{down} = m_i n = \eta_{v,i} \rho_i V_i n \qquad (15)$$

Though the expression for capacity is rather simple, it is still quite complicated to determine the value of the specific mass flow for the reason that we do not know the value of the volumetric filling ratio. The specific mass flow cannot be directly calculated due to the dependency between bulk density and size distribution. Therefore, an iterative and recursive calculation procedure is needed.

10.2 VOLUMETRIC FILLING RATIO

The volumetric filling ratio $\eta_{v,i}$ describes to what extent the accessible zone volume is filled. The value of $\eta_{v,i}$ varies from zone to zone. If the filling ratio of the inlet zone could be determined, the specific mass flow could also be calculated. It would then be possible to calculate the corresponding value of η_v for the other zones. The specific mass flow of course remains constant between the crushing zones. Otherwise, mass continuity would not be preserved.

The volumetric filling ratio depends on several factors. It is affected by the design of the crusher inlet, rheology of the feed material, size distribution (especially in relation to the inlet opening), moisture content, etc. The value of the filling ratio is a measure of how much air there is in the rock material aggregate to be crushed. For the application studied, the value of η_v has been found to be significantly below one. The possibility to decrease the closed side setting of the crusher is determined by the value η_v. A low value of η_v corresponds to a large proportion of air, which in turn allows a relatively small value of the closed side setting CSS.

If the feeding conditions were altered such that the filling ratio was increased, the capacity of the crusher would increase in theory. On the other hand, if the feeding of the inlet zone was made more efficient, the packing density might be exceeded at some stage. Thereby the closed side setting would have to be increased, leading to a decreased overall size reduction. This phenomenon has been observed in operating crushers [28] and is not always a desired effect.

It is assumed that small changes in closed side setting do not affect the filling ratio for the inlet zone. Test results for a crusher operating on the limit to packing can therefore be used to

calibrate the filling ratio for the inlet zone. During the simulations with different closed side settings the value of η_v was kept constant independently of the closed side setting. If no full-scale tests are available for calculating the volumetric filling ratio, the inlet of the crushing chamber needs to be modelled in detail.

The direction of interdependence between the parameters involved in the size reduction predictions is shown in Figure 24. The density of the material entering the first zone is known, as it is equal to the uncompressed bulk density $\rho_{1,u}$ of the incoming feed material. Of all crushing zones, only one single zone can control the final capacity. A recursive type of calculation scheme is needed to find this zone.

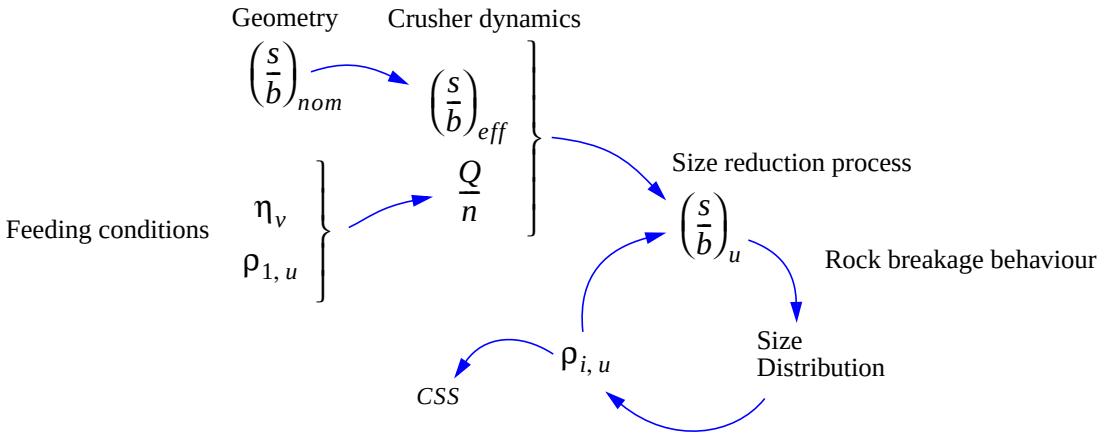

Figure 24. Direction of interdependence for a size reduction cycle.

A condition which must be fulfilled to avoid packing is that the density after every compression step must be lower than the solid density ρ_s.

$$\rho_{i,\,compressed} < \rho_s \tag{16}$$

The maximal possible compression ratio is achieved when all air is compressed out of the aggregate system. Packing will be avoided as long as the following condition is fulfilled:

$$\left(\frac{s}{b}\right)_u < \left(1 - \frac{\rho_i}{\rho_s}\right) \tag{17}$$

The packing condition must be checked for every crushing zone. If the condition is fulfilled, the calculation may proceed with size reduction and then continue with the next zone. If the condition is violated, the value of the volumetric filling ratio has to be decreased, and we have to start it all over again with zone number one. The calculation procedure is shown in Figure 25.

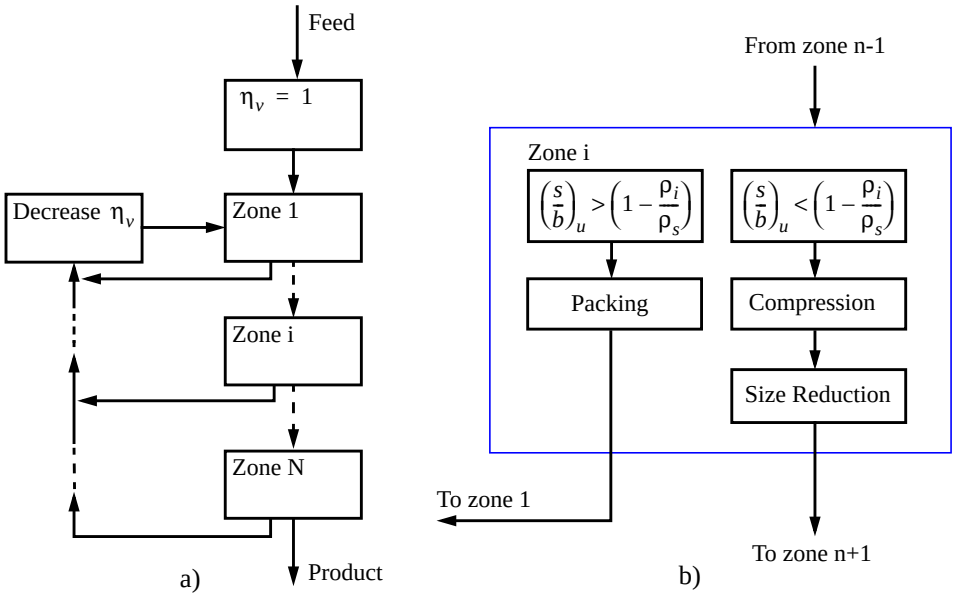

Figure 25. The iterative and recursive calculation procedure used for determination of the volumetric filling ratio.

10.3 UTILIZED COMPRESSION RATIO

Due to the volumetric filling ratio, only a fraction of the total nominal stroke will be utilized for size reduction. A part of the effective stroke will act as an idling stroke. Size reduction cannot begin until the uncompressed density of the aggregate is reached.

The *nominal* compression ratio $(s/b)_{nom}$ is given from the geometric analysis of the crushing chamber based on design drawings. The *effective* compression ratio $(s/b)_{eff}$ corresponds to the ratio which is possible to utilize after considering crusher dynamics. The *utilized* compression ratio $(s/b)_u$ is less than the effective ratio and is a result of mass continuity and requirements such as packing. The relation between nominal, effective and utilized compression ratio is therefore:

$$\left(\frac{s}{b}\right)_u < \left(\frac{s}{b}\right)_{eff} < \left(\frac{s}{b}\right)_{nom} \tag{18}$$

In Figure 26 a schematic representation of a crushing zone is shown. After taken the idling stroke s_t into account, the utilized compression ratio $(s/b)_u$ can be calculated.

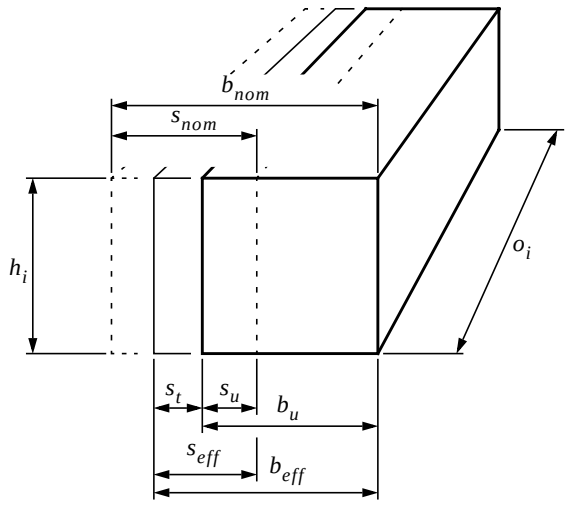

Figure 26. A schematic representation of a crushing zone.

The utilized bed thickness can be calculated from the specific mass flow Q/n, density ρ_i, crushing zone height h_i and zone circumference o_i

$$b_u = \frac{Q}{n} \cdot \frac{1}{\rho_i} \cdot \frac{1}{h_i o_i} = \frac{\eta_{v,1}\rho_1 V_1}{\rho_i} \cdot \frac{1}{h_i(2\pi R_i)} \tag{19}$$

The utilized stroke can then be calculated:

$$s_u = s_{eff} - b_{eff} + b_u \tag{20}$$

Finally, the utilized compression ratio is obtained as the ratio between utilized stroke and bed thickness:

$$\left(\frac{s}{b}\right)_u = \frac{s_u}{b_u} \tag{21}$$

10.4 RELATION BETWEEN BULK DENSITY AND SIZE DISTRIBUTION

A model which relates size distribution width to uncompressed bulk density of aggregates is needed for the calculations, as the density will vary between the crushing zones. The density model developed was calibrated using results achieved from full-scale crushing tests, see Figure 27a (*Paper D*). To make the size distribution model independent of the specific rock type, a normalized density $\rho_{\aleph}$ was introduced. The normalised density is achieved by dividing the uncompressed bulk density of the aggregate ρ achieved from the tests by the solid density of the rock material ρ_s. The measured relationship between normalized size distribution and normalized density is shown in Figure 27b.

$$\rho_{\aleph} = \frac{\rho}{\rho_s} \tag{22}$$

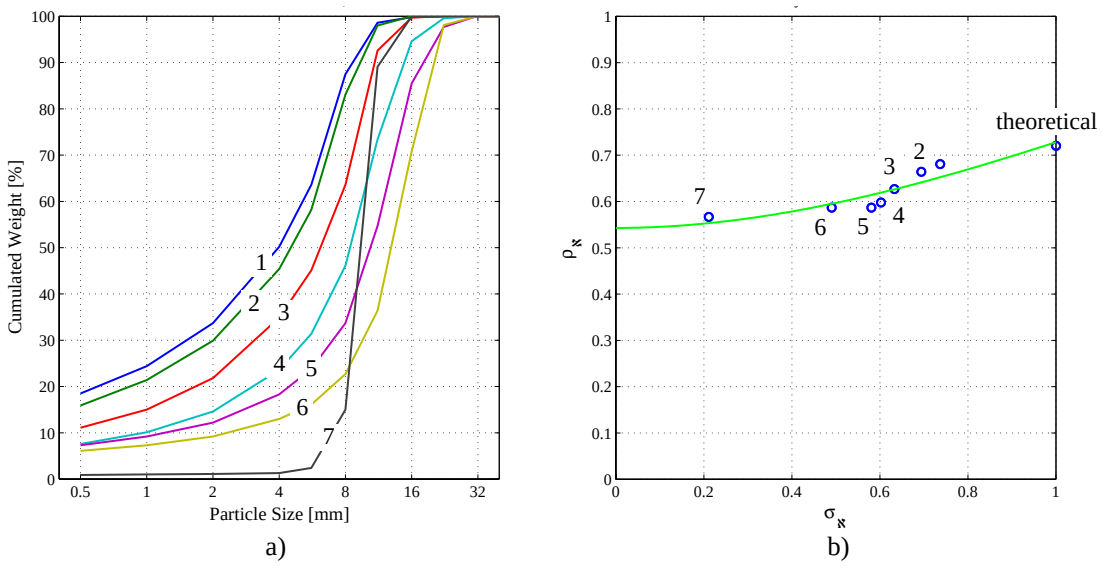

Figure 27. a) Product size distributions used to calibrate the density model for gneiss. b) Normalized density as a function of normalized size distribution width.

The use of typical size distributions originating from full-scale tests implies that the model is valid in the region of practical interest. However, it was found during the size reduction simulations that wider size distributions could be achieved than the ones achieved from full-scale tests. For this reason, a theoretical point with $\sigma_{\aleph} = 1$ was introduced, corresponding to the widest possible size distribution.

The relation between $\rho_{\aleph}$ and $\sigma_{\aleph}$ is assumed to follow the expression given in Eq. (23), which was fitted to the experimental data.

$$\rho_{\aleph} = D_1\sigma_{\aleph}^3 + D_2\sigma_{\aleph}^2 + \rho_{\aleph,\,\mathrm{mono}} \tag{23}$$

The constant $\rho_{\aleph,\,\mathrm{mono}}$ corresponds to the normalized density of an aggregate with a very narrow size distribution, i.e. a mono-size distribution with $\sigma_{\aleph} = 0$. After fitting Eq. (23) to the test results, the following values of the parameters were achieved (*Paper E*)

$$\rho_{\aleph,\,\mathrm{mono}} = 0.54284 \qquad D_1 = -0.062277 \qquad D_2 = 0.24758$$

The normalized test results from the density measurements together with the adapted data are shown in Figure 27b.

10.5 CONFINEMENT AND BREAKAGE MODES

Confined conditions are required if interparticle breakage is to occur when a bed of particles is compressed. The particle bed could either be fully or partly confined. If no confinement at all is achieved then only single particle breakage can occur.

For choke-fed conditions, the inlet zone together with the zones down to and including the choke zone will be choke fed and therefore also confined. This implies that interparticle breakage occurs. Single particle breakage will also occur for particles with a particle size larger than the local closed size setting. For the crushing zones below the choke zone the volume increase makes the forming of confined particle beds unlikely. Therefore, it is assumed

that only single particle breakage will occur in these zones.

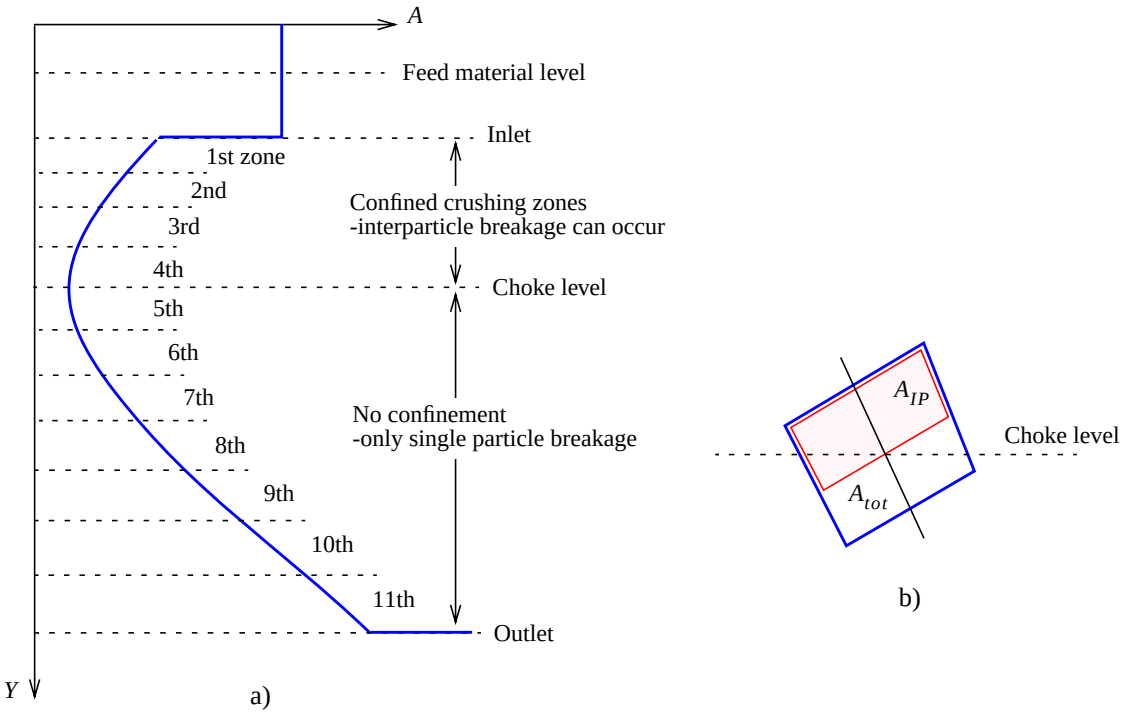

Figure 28. a) General appearance of the horizontal cross-sectional area of a crusher. b) A Crushing zone which is cut by the choke level.

Considerable proportions of interparticle breakage in the lowest zones would only be possible under the conditions that the material flows in rills. This type of flow seems very unlikely to occur, which implies that forming of particle beds is rare and thus very little interparticle breakage occurs.

The number of crushing zones does not necessarily need to be an integer number. If the choke level cuts through a crushing zone, interparticle breakage is only achieved in the upper part of the crushing zone and single particle breakage in the lower part, see Figure 28b. The amount of interparticle breakage ξ_{IP} is assumed to be equal to the ratio between the area of the upper part and the total area of the crushing zone.

$$\xi_{IP} = \frac{A_{IP}}{A_{tot}} \tag{24}$$

The product size distribution descending from the partly confined zone will be a mix of particles originating from interparticle breakage and single particle breakage:

$$\mathbf{p} = \xi_{IP}\mathbf{p}_{IP} + (1 - \xi_{IP})\mathbf{p}_{SP} \tag{25}$$

10.6 CHOKE FEEDING

Over the years the idiomatic expression *choke feed* has been established to describe the feeding conditions for a cone crusher. A choke fed crusher is a crusher with an inlet totally covered with feed material. The common opinion is that choke fed conditions are vital for achieving interparticle breakage, which in turn is a breakage mode that governs good particle shape.

A common solution for achieving choke feeding is to use a small bin on top of the crusher.

The level of the feed material is kept between an upper and a lower limit by some control device. This type of solution inherently assumes that the feeding conditions are not affected by the pressure exerted by the material volume above the inlet (cf. pressure in fluids). There are examples where the level of the material surface in the bin affects the crushing parameters leading to variations in the final product [28].

The author agrees with the statement that choke feeding is necessary for achieving a stable feed (stationary) to the inlet of the crusher. A stable feed guarantees minimal variations in the final product. However, the currently used definition of choke fed conditions might not be a sufficient requirement to achieve proper feeding conditions. The pressure exerted by the bulk material in the bin on top of the crusher will affect the volumetric filling ratio as well as the confinement of the first crushing zone. Requirements on the feed material level may also be necessary.

10.7 A PARTICLE SHAPE MODEL FOR SINGLE PARTICLE BREAKAGE

From a simulation point of view, there is a great difference between interparticle and single particle breakage concerning particle size. In the calculations, all particles will be treated independently of particle shape, as if they were one-dimensional. To handle the shape problem a shape model describing the distribution of the variation in geometry is needed.

A problem arises when simulations are compared with results from sieving. Up until now the crushing simulations are one dimensional while sieving is a two-dimensional method. Obviously, to compare simulations with sieving requires some extra care.

For interparticle breakage, the local closed side setting, i.e. the distance between mantle and concave, is always larger than the particle size. The particles originating from interparticle breakage will have no geometric calibration in terms of particle size. By definition, in the case of single particle breakage, the local closed side setting is always smaller than the particle size. The particle will be in contact with both mantle and concave. The resulting product is thereby calibrated by the crusher.

In reality, there is always some amount of over-sized material compared to the closed side setting at the crusher outlet. A minor amount of this material might originate from a crushing zone located a distance upstream the crushing chamber. The major part of the over-size is explained by the fact that the single particle breakage mode generates miss-shaped particles. Such a particle can have a smallest size t which is calibrated by the local closed side setting of the crusher, while it also has a width d which can be significantly larger, see Figure 29. At sieving, such a particle will appear as a particle of size d, while it was treated as a particle of size t during the simulations.

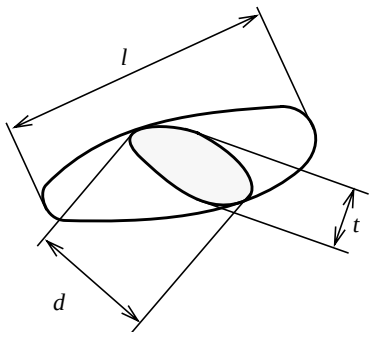

Figure 29. An elongated particle where t<d<l.

One way to eliminate the problem would be to perform single particle breakage tests. The

breakage function describing single particle breakage would then be achieved by laboratory sieving. Miss-shaped over-sized particles would then inherently be included in the breakage function. In this work the breakage function achieved from the interparticle compressing crushing tests is intended to be used. As these tests are purely interparticle, a model capable of estimating the over-sized material is needed. Here it is assumed that a fraction γ of the particles broken in the single particle mode is elongated. Further, it is assumed that the geometry of these flaky particles can be approximated with a ratio between particle width d and thickness t, which is denoted λ.

$$\lambda = \frac{d}{t} \tag{26}$$

Single particle breakage will occur if the thickness of a particle is greater than the local closed side setting.

$$t = \frac{d}{\lambda} > CSS_{local} = b - s \tag{27}$$

This condition is valid for nominal, effective and utilized bed thickness and stroke, see Figure 26.

Further, the compression ratio, which a particle of size d is exerted to, is

$$s_{\text{א, single}} = 1 - \frac{\lambda(b-s)}{d} \tag{28}$$

The values of the parameters in the particle shape model chosen are $\lambda = 2$ and $\gamma = 0.5$. The expression describing the size reduction is achieved by modifying Eq. (3). The expression now consists of two parts, one for the flaky and one for the non-flaky cubical particles.

$$\begin{aligned}\mathbf{p}_{i+1} = {} & \gamma\{[\mathbf{B}_i^{\text{inter}}\mathbf{S}_i + (\mathbf{I} - \mathbf{S}_i)]\mathbf{M}_i^{\text{inter,flaky}} + \mathbf{B}_i^{\text{single,flaky}}\mathbf{M}_i^{\text{single,flaky}}\}\mathbf{p}_i + \\ & (1-\gamma)\{[\mathbf{B}_i^{\text{inter}}\mathbf{S}_i + (\mathbf{I} - \mathbf{S}_i)]\mathbf{M}_i^{\text{inter}} + \mathbf{B}_i^{\text{single}}\mathbf{M}_i^{\text{single}}\}\mathbf{p}_i\end{aligned} \tag{29}$$

11 SIMULATION RESULTS AND EXPERIMENTS

To validate the crusher flow and size reduction models full-scale tests were performed at realistic operating conditions. During the tests both the eccentric speed and the closed side setting were altered. The crusher chosen for these tests was a Svedala Hydrocone equipped with an fine-crushing chamber.

11.1 ACCURACY

Computed results are rarely exact but if the difference between the computed result and the real behaviour of a system is small enough, the error is of no importance. If there is an unacceptable difference there is also a need to identify the origin of the error.

Modelling errors occur if there is a difference between the physical system and the mathematical model.

Feed and product in the size reduction process are described by size distributions. These distributions are cumulative functions of a linear size of the particles. The use of a *linear* size is perhaps an easy and convenient description but it does not tell anything about the shape of the particles. The linear size is defined by a sieve analysis. The size of a particle is then smaller than the width of a square aperture, which the particle can pass through, and it is larger than a width, which it cannot pass through. Single particles, which are assigned a certain size from the sieve analysis, can have completely different shapes and will therefore also be likely to behave differently during breakage.

There is also a loss in accuracy in the transformation from the sieve analysis data to the frequency vector, which is used to characterize the feed material coming to the reduction process. The approximation of a continuous distribution by a discrete vector will therefore give rise to a *discretization error* which has been obvious when working with this project.

11.2 FLOW

Simulations of particle flow are conducted in *Paper D*. In the simulations the time delay t_d was set to 0.01 second. The simulated vertical position of a particle starting from the choke-level is shown in Figure 30. The predominant flow mechanism is free fall. Sliding occurs only at low eccentric speed. The total covered distance in the vertical direction decreases with increasing eccentric speed. One notice that if the nominal stroke is to be fully utilized the eccentric speed chosen should be just below 300 rpm.

The velocity distributions are shown in Figure 31. The influence of the constant time delay on velocity is clearly seen. The velocities in the upward direction are substantial compared with the ones in the downward direction. However, the upward velocities should be divided by a factor of two before comparison, as the velocities on the concave surface have zero velocity. In Figure 32 the velocities are shown in a polar plot. Here it is clearly demonstrated how the eccentric angles are utilized. For the lowest speed the nominal stroke is fully utilized while for the highest only half of the nominal stroke is utilized.

By repeated simulations it is possible to show how a particle is transported through the crusher chamber. As the predominant flow mechanism is free fall, this simulation will give us the fastest possible way a particle can take. The resulting path of a repeated simulation is shown in Figure 33. For a given eccentric speed the height of the crushing zones does not seem to change significantly. With increasing eccentric speed the number of crushing zones increases. The effective bed thickness and stroke decreases when the eccentric speed increases.

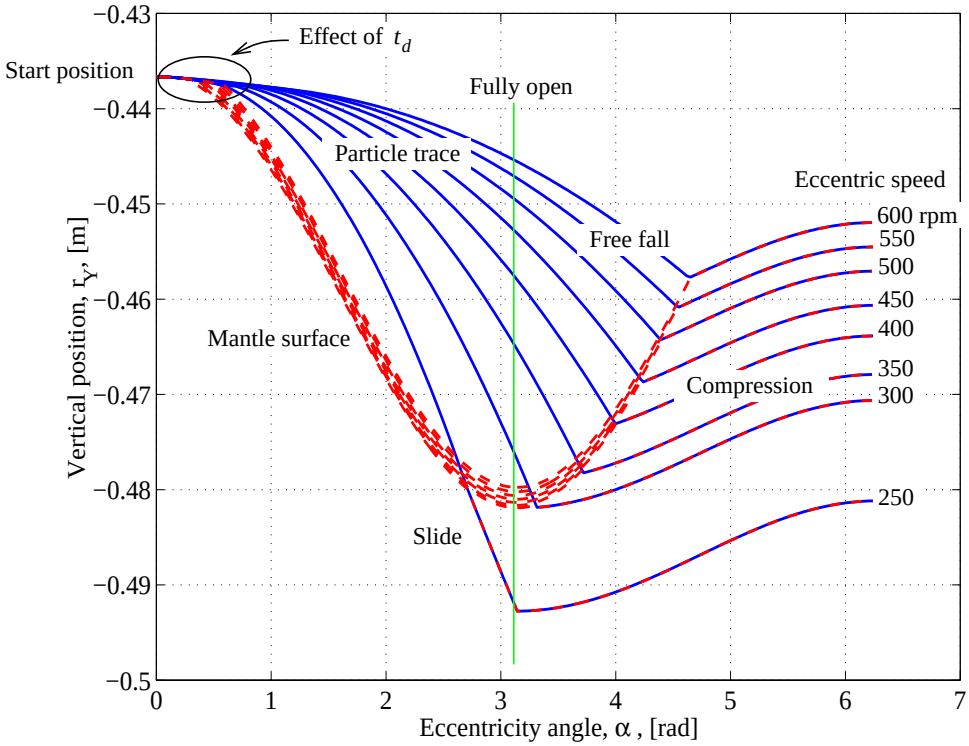

Figure 30. Simulated vertical position of a particle at different eccentric angles. For the studied crusher, free fall is the predominant flow mechanism (t_d = 0.01 s).

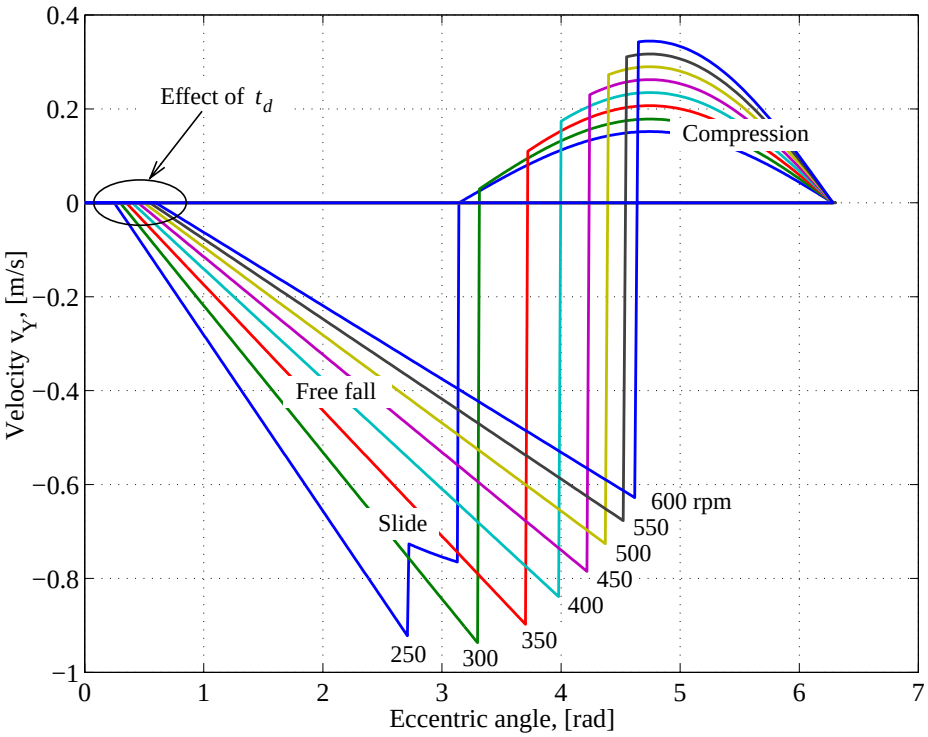

Figure 31. Velocity distributions in the vertical direction at choke-level (t_d = 0.01 s).

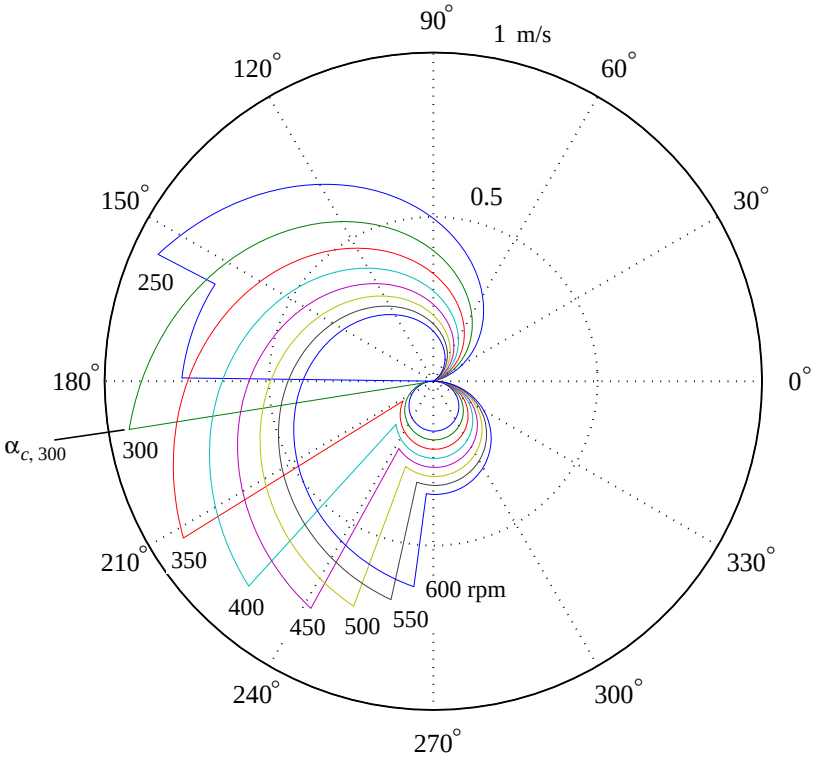

Figure 32. Polar plot showing the magnitude of the velocity distributions in vertical direction at choke-level (t_d = 0.01 s).

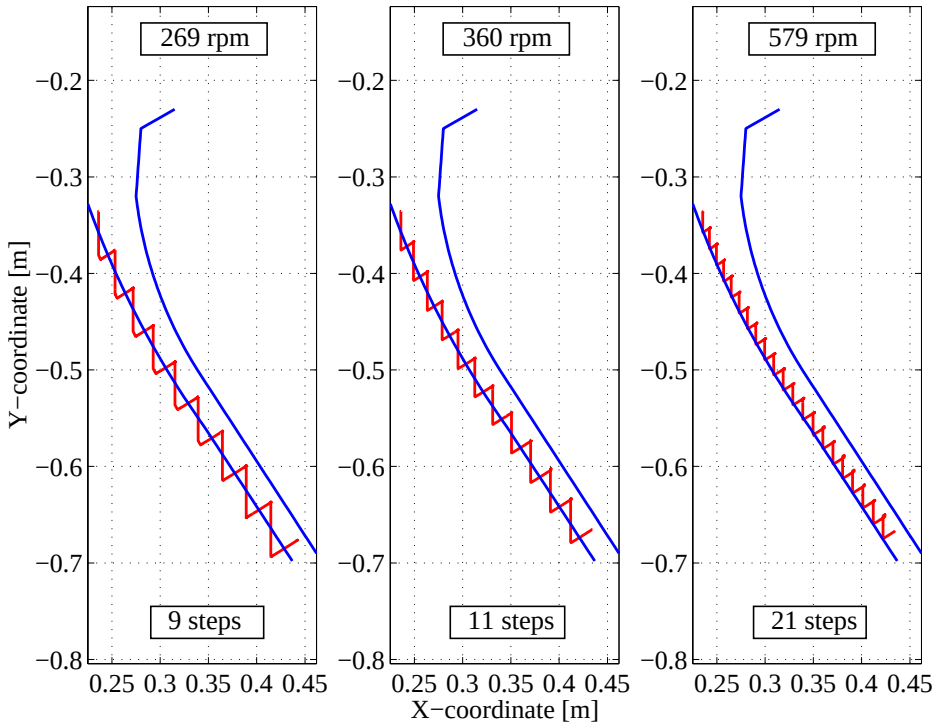

Figure 33. Repeated simulations show how a particle is transported through the crusher chamber. When the eccentric speed increases the number of crushing zones increases.

11.3 SIZE REDUCTION

Size reduction simulations were conducted in *Paper E*. Size distribution tests were performed at the same time as the flow tests. The simulations started with calibration of the volumetric filling ratio η_v according to Figure 25. From the full-scale tests it was found that packing occurred at a closed side setting of 7.2 mm. The volumetric filling ratio of the inlet zone were determined to be 0.70 for this case. For the simulations η_v was assumed to be constant independently of the closed side setting.

Simulated results, together with measured feed and product size distributions for three different eccentric speeds and for two different closed side settings, are shown in Figure 34. The same cases but in more detail, with the size distributions after each reduction event, are shown in Figure 35. The corresponding compression ratios are shown in Figure 36.

The model response to changes in closed side setting matches the full-scale tests very well. The number of interparticle crushing zones (*#IP)* decreases when the closed side setting increases. This is a consequence of an upward movement of the choke level with increasing CSS. The effect is strongly dependent on the specific design and is therefore not necessarily a general behaviour for cone crushers. The most important effect associated with increasing CSS is a decreasing compression ratio. When compression ratio decreases, the overall size reduction also decreases. This effect is obvious, but has never been proven by this type of simulation before. The combined effect of decreasing number of crushing zones and compression ratio is an overall decrease in size reduction.

The model response when the eccentric speed is changed is very interesting but difficult to interpret. Due to the relatively small difference in overall size reduction for both simulations and for full-scale tests it is difficult to draw quantitative conclusions by only comparing the size distributions for the resulting product, see Figure 34. However, by studying how the size distributions evolve from each crushing event, considerable differences are discovered. The number of interparticle crushing zones increases significantly when the eccentric speed increases. Simultaneously, the compression ratio decreases as a dynamic effect of increasing speed (*Paper B and E*). Under these conditions it is remarkable that such small differences are achieved for both simulations and full-scale tests. The explanation is probably to be found in the location of the choke level. If the choke level is placed at the outlet of the crushing chamber, a more pronounced dependence on eccentric speed is to be expected (*Paper D*).

The main part of the total size reduction is achieved by interparticle breakage. The number of interparticle breakage events is relatively small in all of the studied cases. A typical number is between 2.5 and 4.5.

After the zones of interparticle breakage and down to the outlet, the breakage mode is purely single particle. Here, the material is mainly calibrated by the crusher, and the resulting size reduction is relatively small in this region. The number of single particle crushing events is between 6 and 10.

In terms of reduction efficiency, the part of the crushing chamber above the choke level is more efficient compared to the lower part. The *calibration zone* is commonly defined as the part of the chamber above the outlet where the profile mantle and concave surfaces are nearly parallel. It is often claimed that the calibration zone governs particle shape. This zone is located below the choke point and thus the breakage mode is single particle. An inappropriate design of the calibration zone can be devastating to particle shape [6].

A closer inspection of the agreement between simulated results and full-scale tests shows a systematic over-prediction of the overall size reduction for the simulation. This is probably an effect which originates in the assumption that the zones where interparticle breakage occurs

are fully confined. If the degree of confinement is lower, the values of the selection and breakage functions will decrease and thus also the overall size reduction.

If repeated size reduction simulations are conducted with different values of one or several parameters the performance behaviour of the crusher is obtained. In Figure 37a size distributions are shown for varying closed side setting. The corresponding Crusher Performance Map is shown in Figure 37b. For comparison, full-scale test results are shown in Figure 38. The similarities between simulations and test results are convincing. The qualitative agreement is especially good in terms of the locations of maximal relative capacities together with the trends of the different fractions.

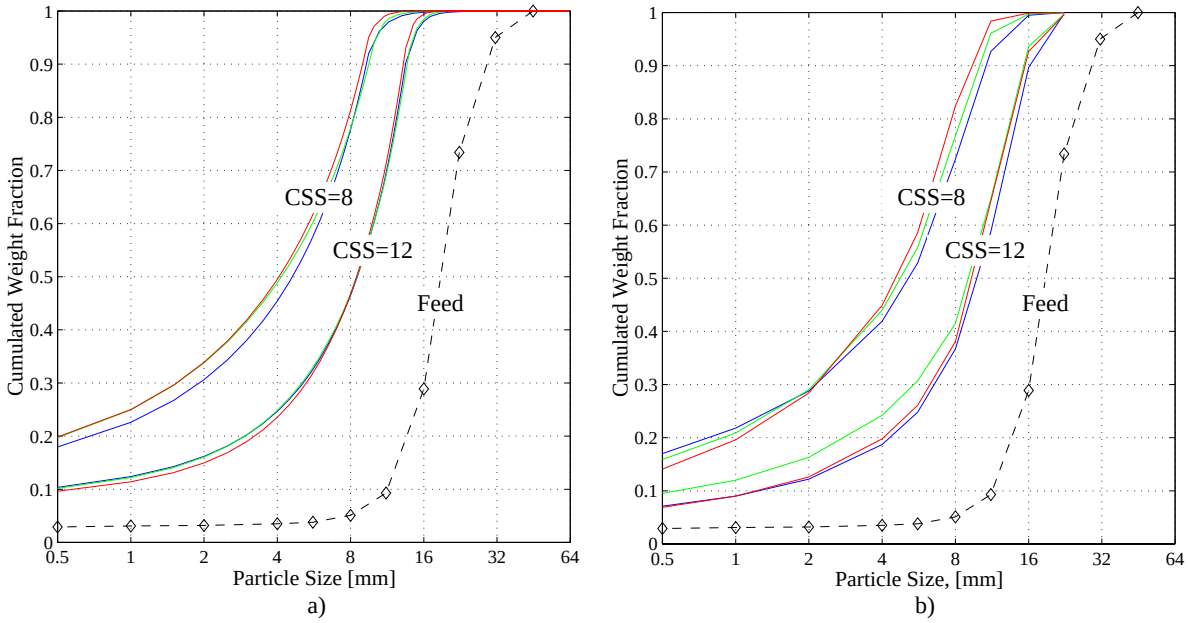

Figure 34. a) Simulated results for three different eccentric speeds and two different CSS. b) Full-scale tests.

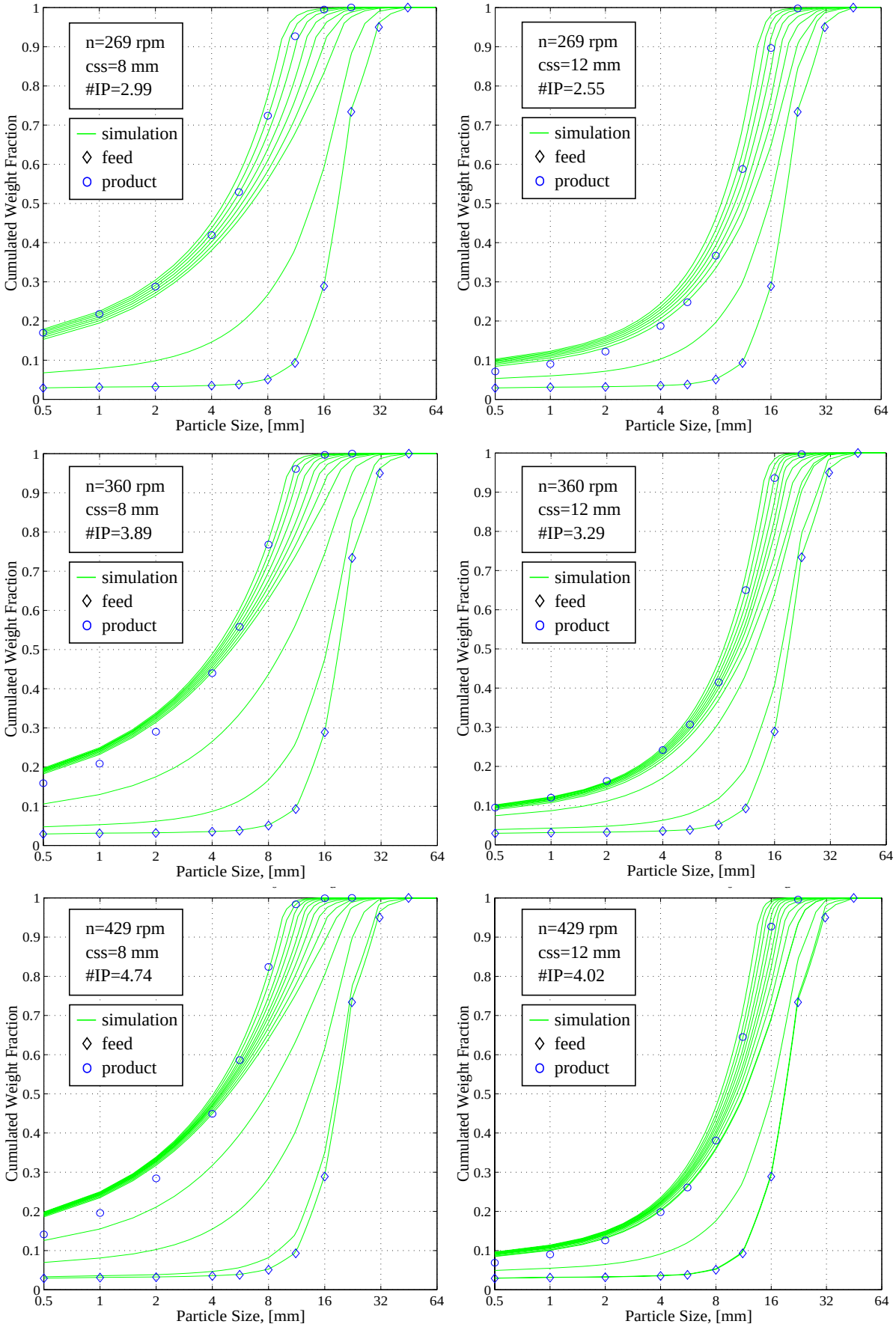

Figure 35. Simulated size distributions after each reduction step for a Svedala Hydrocone.

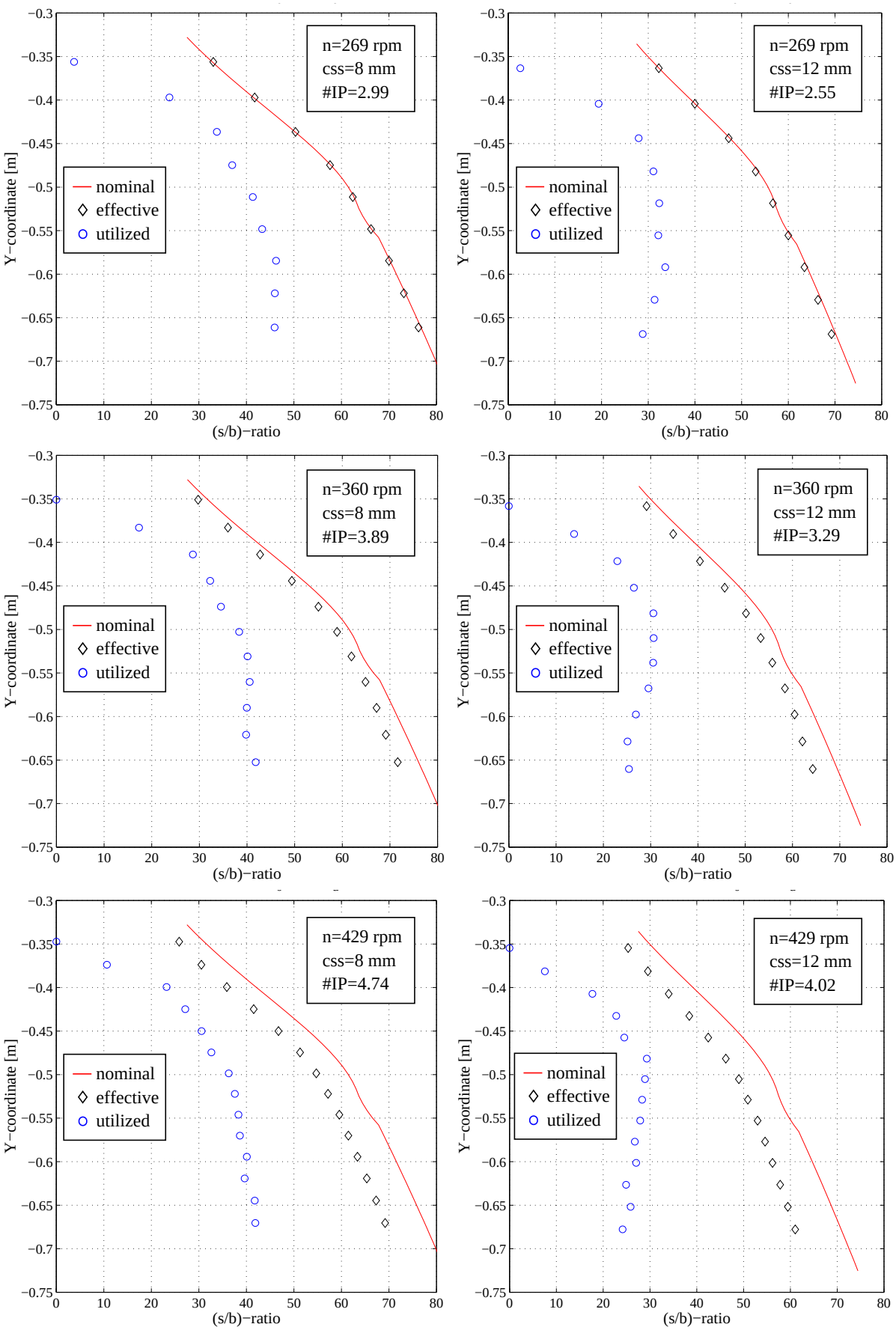

Figure 36. Compression ratios at different settings and speeds originating from simulations for a Svedala Hydrocone crusher.

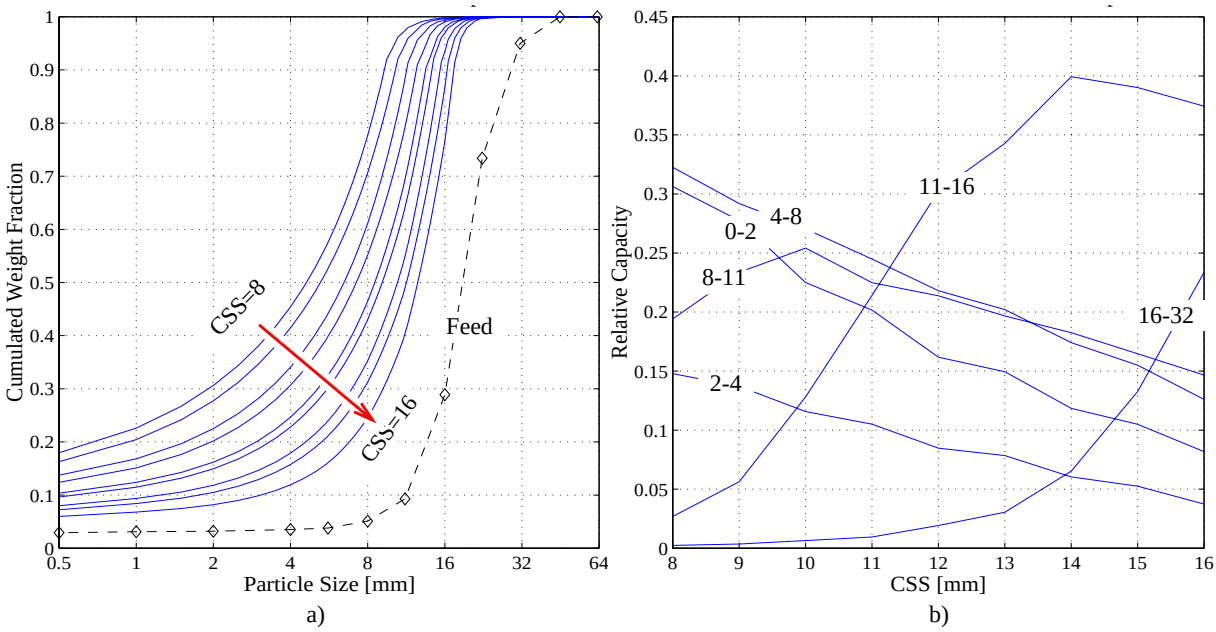

Figure 37. a) Simulated product size distributions at eccentric speed 269 rpm. CSS varies with 1 mm steps between 8 and 16 mm. b) Simulated Crusher Performance Map for eccentric speed 269 rpm.

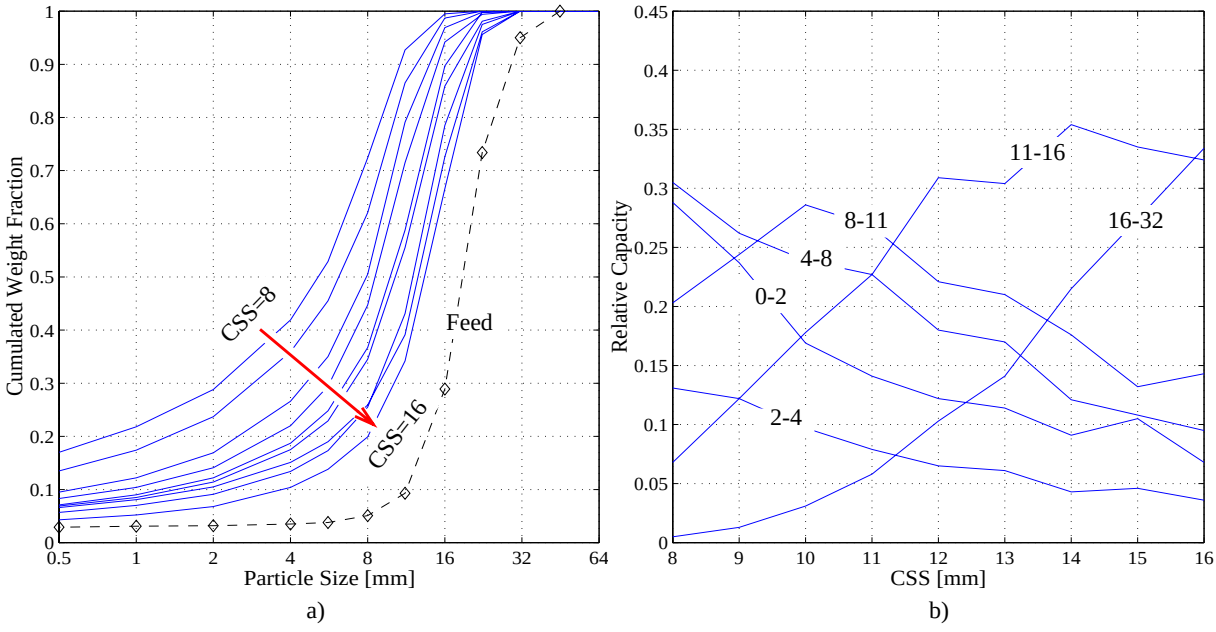

Figure 38. a) Product size distributions from full-scale tests at eccentric speed 269 rpm. CSS varies with 1 mm steps between 8 and 16 mm. b) Crusher Performance Map from full-scale tests at eccentric speed 269 rpm.

11.4 CAPACITY

By integration of the velocity distributions multiplied with the volumetric filling ratio and the density, the total capacities for the different eccentric speeds are obtained. The simulated capacities together with measured are shown in Figure 39. The simulation was conducted with time delay set to 0.01 second and with a filling ratio set to 0.70 as in the size-reduction simulations.

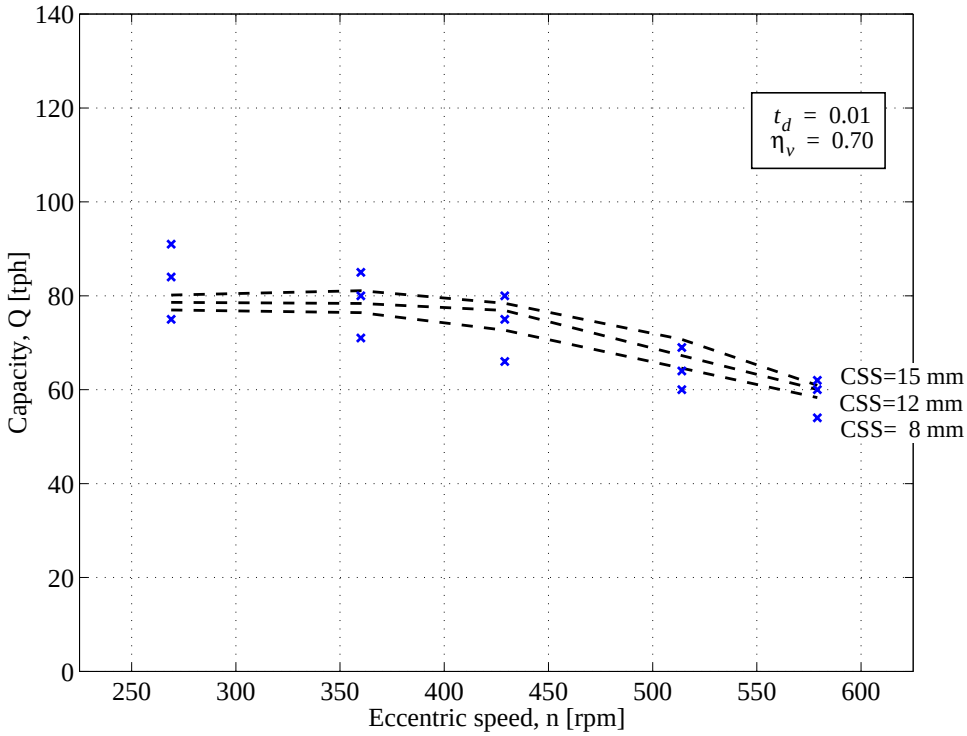

Figure 39. Simulated capacities (lines) compared with full-scale tests (x-marks). The simulated capacities are calculated for three different CSS at the same eccentric speeds as is the full-scale tests (269, 360 429, 514 and 579 rpm).

The capacities were evaluated at the choke level. The volumetric filling ratio of the inlet zone were held constant between the simulations. This implies that the filling ratio at the choke level will vary as the density varies with the size distribution of the material entering this level.

12 DESIGN CONSIDERATIONS

Three *main factors* are identified to promote the size reduction process occurring in a cone crusher, viz. breakage modes, number of crushing zones and compression ratio. These main factors provide a possibility for a fundamental and detailed understanding of how a cone crusher operates. The factors are affected by both design and operating parameters. Any design consideration should be evaluated against the three main factors.

Interparticle breakage governs particle shape whilst single particle breakage is most energy efficient [6]. If a number of interparticle crushing zones is followed by a calibration zone it is strongly recommended that this zone is parallel or slightly divergent. In this way the probability to produce miss-shaped elongated particles close to the crusher outlet is minimized.

The number of crushing zones is controlled by crusher height and eccentric speed. A crusher which has the choke zone relatively high up the chamber could probably be shortened from the bottom with a couple of crushing zones without any significant loss in overall size reduction.

For a crusher with the choke zone near the outlet of the chamber, the first interparticle crushing zones will have very little affect on the size reduction. In these zones the (s/b)-ratios are so low that the value of the selection function will approach zero and thus not contribute to any size reduction.

The compression ratio is mainly controlled by chamber profiles, crusher dynamics and volumetric filling ratio. Together these factors results in the utilized compression ratio $(s/b)_u$. In turn the utilized compression ratio determines the values of selection and breakage.

The breakage behaviour of rock materials seems to be strongly non-linear given the approach in this work. For the gneiss and diabase material studied in *Paper B and E* the combined behaviour of selection and breakage is obviously non-linear, see Figure 16 and 17. It is likely that there exists a “best way” to achieve a desired size reduction. This way could be formulated as a *size reduction strategy*. The size reduction strategy comprises the optimal choice of (s/b)-ratios, number of crushing events and breakage modes.

The optimal size reduction could be found by iterative calculations in which the selection and breakage functions are utilized. The size reduction strategy is achieved by the crusher machine as shown in Figure 40. For a given crusher concept, e.g. a cone crusher, there will be theoretical limitations in that is possible to achieve. In a case where the crusher concept limits the size reduction strategy there will be a potential for innovations. New crusher types could be synthesized originating from the strategy.

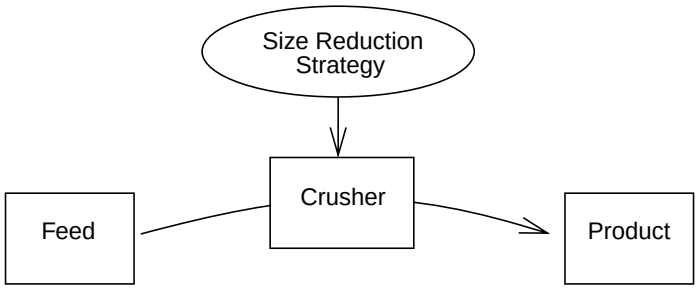

Figure 40. A size reduction strategy can be applied to the transformation of the feed to the product.

13 CONCLUSIONS

13.1 GENERAL

A calculation method with a modular structure based on a deductive crusher model has been developed. The presented model is a comprehensive analytical tool for predicting cone crusher performance and provides detailed understanding of how and where size reduction is achieved in a cone crusher. Full-scale tests has been performed to validate the model. The agreement between simulated results and experimental data is very good. The model is capable of establishing a direct correlation between crusher design parameters, rock fragmentation behaviour and crusher performance. The model can be used as a simulation tool to assist in the design process of cone crushers. Any arbitrary design can then be studied.

In the crusher model there are only two parameters which are unknown and has to be tuned. The time delay parameter t_d is used to compensate for varying moisture content. The volumetric filling ratio η_v is determined by iterative calculations in which the packing criteria is checked.

Data governing the detailed understanding of how a cone crusher works is achieved from the simulations. Detailed information about how different machine parameters affect the size reduction process in every crushing zone is provided by the model. Different crusher behaviours can be explained depending on crusher layout. The identity of a crusher brand or model can be characterized by a couple of crusher related parameters. Different machine layouts can be compared and evaluated early at the design stage. Improvements in crusher design can be done without excessive testing.

Three *main factors* are identified to promote the size reduction process occurring in a cone crusher. These factors are: breakage modes, number of crushing zones, and compression ratio. The main factors are affected by both design, rock material and operating parameters. For a given crusher application, the factors depend on eccentric speed, closed side setting and feed size distribution. The main factors provide the possibility for fundamental and detailed understanding of how a cone crusher operates. Any design consideration should be evaluated against these three main factors.

If a set of simulations is performed for a given crusher, a *Crusher Performance Map* is achieved, which in turn can be used when optimizing a given crushing task or a crushing plant. The Crusher Performance Map describes how the product output from the crusher varies with machine parameters. By applying optimization criteria to the Crusher Performance Map the best operating conditions can be found. It appears that the output from a tentative cone crusher strongly depends on the eccentric speed. For the studied crusher the dependence with eccentric speed was vague

The cone crusher performance model gives manufacturers the possibility to tailor make customized crushing chambers. With the three main factors as design considerations new crushing chamber geometries can be synthesized to fulfil the desired behaviour of the crusher. Desired values of the main factors are in turn achieved by choosing correct values of the design and operational parameters. The potential for improvements is high and therefore also of great interest for the industry. The improved understanding of the size-reduction process also governs the possibility for synthesis of knew crusher concepts.

13.2 FLOW

From the derivation of the flow model together with simulated results, a number of interesting conclusions can be drawn. The validity of the flow model is achieved through the agreement between simulated results and full-scale test data. Especially, the response of the model to changes in closed side setting is very promising. In turn, this fact verifies that the cross-sectional area at the choke-level is the controlling factor of the overall capacity.

The flow model provides a fundamental understanding of the flow mechanisms occurring in a cone crusher. These mechanisms have earlier been described only briefly.Free fall is the predominant flow mechanism at typical eccentric speeds. Standard eccentric speeds chosen by crusher manufacturers seem not to fully utilize the nominal stroke at the choke point. The choice of a specific eccentric speed is probably empirically found and reflects the complex situation between crusher capacity and overall size reduction.

The simulations show that there is a substantial flow of material upwards due to the *uplift*-effect. This upward flow of material will reduce the overall capacity and cannot be ignored. The same effect is necessary for the horizontal (radial) transport of the material from the inlet to the outlet of the crushing chamber.

By simulating the fastest way through the crusher it is shown that the number of crushing zones is about twice as high than previously believed.

13.3 SIZE REDUCTION

The size reduction model is based on the laws of mechanics and constitutive relations concerning rock breakage characteristics. There are some crucial assumptions which are of central interest for the model. The validity of these assumptions are verified by full-scale tests.

Early in the development of the crusher model it was claimed that the overall size reduction process is a result of several subsequent crushing events. Regarding the process model, an important property is that it must be closely physically defined. This is guaranteed by modelling size reduction in a cone crusher as a repetitive process.

Each crushing event is modelled with a selection and a breakage function. The appearance of the selection and breakage functions is rock material specific and can be obtained by laboratory tests. The fact that laboratory tests can be utilized for prediction of cone crusher performance is important and will in time reduce the need for full-scale testing.

Two different modes of breakage are possible to achieve in a cone crusher. The criterion determining which breakage mode acts where is the location of the choke level. The dominating breakage mode above the choke level is interparticle breakage while mostly single particle breakage is achieved below this level.

13.4 FUTURE WORK

There are numerous improvements and extensions that can be made in the future. At present the simulation tool is able to predict both crusher capacity and product size distribution from cone crushers. There are no inherent limitations to extending the model to also predict other desired features, such as product quality, crusher wear and power consumption.

Formulation of size reduction strategies will further gain the fundamental understanding of the size reduction process. The size reduction process does not necessary need to utilized form conditioned compressive crushing, but could use any comminution principle.

REFERENCES

[1] Barnard, W. J. and Bull, F. A., “Primary Breakage of Brittle Particles”, *Fourth Tewksbury Symposium*, Melbourne, Australia, February 1979.

[2] Bearman, R. A., “The Application of Rock Mechanics Parameters to the Prediction of Crusher Performance”, *Ph.D. Thesis*, Camborne School of Mines, England, 1991.

[3] Bond, F. C., “Third Theory of Comminution”, *Min. Eng. Trans. AIME*, Vol. 193, 484-494, 1952.

[4] Briggs, C. A. and Bearman, R. A., “An Investigation of Rock Breakage and Damage”, *Minerals Engineering*, Vol. 9, 489-497, May 1996.

[5] Briggs, C. A, “Fundamental Model of a Cone Crusher”, *Ph.D. Thesis*, University of Queensland, Australia, July 1997.

[6] Briggs, C. A. and Evertsson, C. M., “Shape Potential of Rock”, *Minerals Engineering*, Vol. 11, 125-132, February 1998.

[7] Broadbent, S. R. and Callcott, T. G., “Coal Breakage Processes, I. A New Analysis of Coal Breakage Processes”, *J Inst Fuel*, 524-528, December 1956.

[8] Broadbent, S. R. and Callcott, T. G., “Coal Breakage Processes, II. A New Analysis of Coal Breakage Processes”, *J Inst Fuel*, 528-539, December 1956.

[9] Buss, B., Hanische, J. and Schubert, H., “Über das Zerkleinergungsverhalten seitlich begrenzter und nicht-begrenzter Kornschichten bei Druckbeanspruchung”, *Neue Bergbautechnik*, 12, (5), 277-283, 1982.

[10] Eloranta, J., “Influence of Crushing Process Variables on the Product Quality of Crushed Rock”, *Ph.D. Thesis*, Tampere University of Technology, Tampere, Finland, 1995.

[11] Evertsson, C. M., “Prediction of Size Distributions from Compressing Crusher Machines”, *Proceedings EXPLO 95 Conference*, Brisbane, 173-180, 4-7 September 1995.

[12] Evertsson, C. M., “Prediction of Cone Crusher Performance”, *Lic. Eng. Thesis*, Machine and Vehicle Design, Chalmers University of Technology, Göteborg, Sweden, January 1997.

[13] Evertsson, C. M. and Bearman, R. A., “Investigation of Interparticle Breakage as Applied to Cone Crushing”, *Minerals Engineering*, Vol. 10, 199-214, February 1997.

[14] Evertsson, C. M., “Output Prediction of Cone Crushers”, *Minerals Engineering*, Vol. 11, 215-232, March 1998.

[15] Evertsson, C. M., “Modelling of Flow in Cone Crushers”, *Minerals Engineering*, Vol. 12, 1479-1499, December 1999.

[16] Evertsson, C. M., “Size Reduction in Cone Crushers”, *Minerals Engineering Conference '99*, Falmouth, England, 22-24 September 1999, (*Accepted for publication in Minerals Engineering*).

[17] Gauldie, K., “Performance of Jaw Crushers”, *Engineering*, 456-458, October 9, 485-486, October 16, 1953.

[18] Gauldie, K., “The Output of Gyratory Crushers”, *Engineering*, 557-559, April 30, 1954.

[19] Gilvarry, J. J., “Fracture of Brittle Solids, I. Distribution Function for Fragment Size in Single Fracture (Theoretical)”, *J Applied Physics*, Vol. 32, 391-399, March 1961.

[20] Griffith, A. A., “The Phenomena of Rupture and Flow in Solids”, *Phil Trans Royal Soc*, Vol. 7, 29-36, 1933.

[21] Heikkilä, P., “Improving the Quality of Crushed Rock Aggregate”, *Ph.D. Thesis*, Helsinki University of Technology, Helsinki, Finland, 1991.

[22] Hultén, J., “Drum Brake Squeal”, *Ph.D. Thesis*, Machine and Vehicle Design, Chalmers University of Technology, 1998.

[23] Kick, F., “Contribution to the Knowledge of Brittle Materials”, *Dinglers Journal*, Vol. 247, 1-5, 1883.

[24] Klimpel, R. R. and Austin, L. G., “The Statistical Theory of Primary Breakage Distribution for Brittle Materials”, *Trans. SME/AIME*, 232, 88-94, 1965.

[25] Kojovic, T., “Crushing Aggregate and Shape Control”, Quarry Australia, 24-34, June 1995.

[26] Liu, J. and Schönert, K., “Modelling of Interparticle Breakage”, Preprints of 8th European Symposium on Comminution, Stockholm, Sweden, 102-115, May 10-12, 1994.

[27] Lynch, A. J., *Mineral Crushing and Grinding Circuits*, Elsevier Scientific Publishing Company, 1977.

[28] Nilsson, A., Personal communication, Svedala, 1999.

[29] Prasher, C., L., “Crushing and Grinding Process Handbook”, John Wiley and Sons Ltd., 1987.

[30] Rittinger, P. R. von, *Lerbuch der Aufbereitungskunde*, Ernst and Korn, Berlin, 1867.

[31] Rose, H. E., “Drop Weight Tests as the Basis for Calculations of the Performance of Ball Mills”, *Proc. 10th Int. Miner. Process. Congr.*, London, Publ. IMM (London), 143-147, April 1973.

[32] Rosin, P. and Rammler, E., “The Laws Governing the Fineness of Powdered Coal”, *J Inst Fuel*, Vol. 7, 29-36, 1933.

[33] Schönert, K., “Aspects of the Physics of Breakage Relevant to Comminution”, Proc 4th Tewksbury Symposium, Melbourne, Australia, February 1979.

[34] Whiten, W. J., “The Simulation of Crushing Plants with Models Developed using Multiple Spline Regression”, *J South African Institute of Mining and Metallurgy*, 257-264, May 1972.

[35] Whiten, W. J., “Models and Control Techniques for Crushing Plants”, *Control ’84*, *Minl. Metall. Process*, AIME Annual Meeting, Los Angeles, USA, 217-225, February 1984.